Spring Lake Phosphorus Monitoring 2017-2018: External Loading and Spring Lake Microcystin Study

September 2018

Alan D. Steinman, Michael Hassett, and Maggie Oudsema

Annis Water Resources Institute
Grand Valley State University
Muskegon, MI 49441

Executive Summary

A study was conducted between summer 2016 and summer 2017 to determine phosphorus and nitrogen loads in the Spring Lake watershed, as well as microcystin (a toxin produced by cyanobacteria) concentrations in Spring Lake. A P budget for Spring Lake was constructed with the data.

Mean P concentrations in the Spring Lake watershed tributaries ranged from 15 to 35 µg/L during baseflow and from 65 to 125 µg/L during storm events. Norris Creek had the highest P concentrations and P loads of the tributaries that we sampled; within Norris Creek, P concentrations and loads increased farther up the Creek.

The P budget showed that external loading (including tributaries, atmospheric deposition, septic systems, lawn fertilizer, waterfowl, and shoreland runoff) accounted for ~71% of the P load entering Spring Lake on an annual basis; internal loading accounted for the rest. However, the budget has considerable uncertainty because the septage and lawn fertilizer data are outdated.

Microcystin concentrations have increased ~3-fold since last analyzed in 2006. However, the concentrations are still far below the provisional guidelines for recreational water use established by the World Health Organization.

Recommendations based on this study include: 1) target Norris Creek, in particular, for best management practices (BMPs) to manage the P source(s) in that system; 2) revisit a previously developed flow chart that outlines a BMP selection process for the Spring Lake watershed; 3) update the P budget with more recent information, especially regarding septage and lawn fertilizer loads; 4) develop a computational watershed model (e.g., SWAT) to evaluate different scenarios on land use impacts in the watershed; and 5) include microcystin monitoring in future sampling regimes.

Introduction

Historically, Spring Lake has had some of the highest phosphorus (P) concentrations measured in western Michigan lakes; between 1999 and 2002, total P (TP) levels averaged 100 µg/L and ranged from 6 to 631 µg/L during ice-free periods. In response to concerns from residents regarding impaired water quality, laboratory-based studies to assess internal P loading were conducted in 2003 and 2004 using sediment cores from Spring Lake. Based on these results, it was estimated that internal loading accounted for between 55 and 65% of the TP entering the lake water column on an annual basis, and that an alum application of 24 mg Al/L should be effective at reducing TP release from the sediments (Steinman et al. 2004).

In the fall of 2005, an alum treatment of between 10 and 20 mg/L alum was applied as a liquid slurry to the surface of Spring Lake, in locations where depths were ≥ 15 ft. We measured rates of internal P loading and evaluated ecological effects of the alum application in 2006, ~8 months after treatment. Our results indicated that the alum treatment effectively reduced internal P loading and P concentrations in Spring Lake, although water column TP concentrations still remained above the 25 to 30 µg/L target and overall benthic invertebrate density had been reduced (Steinman and Ogdahl 2008). We repeated our analyses in September 2010 and September 2016, ~5 yr and 11 yr post-treatment. In 2016, overall water column TP concentrations remained significantly lower than the 150 to 300 µg/L concentrations measured before the alum application, but there was a trend of increasing concentrations since 2006, especially in the hypolimnion at the two deeper stations. However, maximum internal P loading rates (based on sediment core incubations) remained low, although higher than 8 months following the alum treatment (Steinman and Ogdahl 2012; Steinman et al. 2018). These results suggest, but are not conclusive, that the alum treatment is starting to lose its effectiveness.

Given these high P concentrations in the water column of Spring Lake, there is concern that continued high P loads are entering Spring Lake from the watershed. As a consequence, AWRI was asked to submit a proposal to monitor nutrient loads from the main tributaries to Spring Lake. In addition, with increasing frequency of cyanobacterial blooms, there is concern about potential toxicity from the cyanotoxin microcystin (MC). In this report, we provide our findings regarding external loading to Spring Lake during June 2017 to June 2018, as well as MC concentrations during summer 2017.

Methods

A total of 7 sites in the upper Spring Lake watershed were monitored monthly during stream baseflow from July 2017-June 2018. Sites were established at 3 sites along Norris Creek (the main tributary of Spring Lake) and at 4 sites on other tributaries (Stevens Creek, Willow Hill Creek, Vincent Creek, and Rhymer Creek) (Table 1, Fig. 1). Additional monitoring events occurred during storm flow conditions (~≥ 0.25 inches of rain proceeded by 72 hours of dry weather) on 4 dates: 8/17/2017, 2/20/2018, 5/3/2018, and 5/31/2018. One rain monitoring event occurred on 10/23/2017 that did not meet storm flow sampling criteria; however, stream discharge was measured regardless due to the magnitude of rainfall in order to improve the hydrologic modeling dataset (methods detailed below; see Table 6). Note that physical and chemical parameters of water quality were not measured during the 10/23 high flow event and are not included in the results summary.

Table 1. Site coordinates for each monitoring location. Sites are shown from downstream to upstream sampling order throughout the watershed (see Fig. 1).

Waterbody	Site ID	Latitude (°N)	Longitude (°W)
Spring Lake	L1	43.08266	86.20326
	L2	43.08872	86.18599
Spring Lake Tributaries	S1	43.13209	86.18503
	WH1	43.13221	86.14864
	V1	43.12138	86.13943
	N1	43.13260	86.12124
	R1	43.14734	86.11933
	N2	43.15414	86.09060
	N3	43.17434	86.06626

A homemade staff gauge, made of PVC pipe and measuring tape, was installed at each tributary site and transects were established upstream of each gauge. Stream stage height was measured during each base and storm flow sampling event and water velocity was measured using a Marsh-McBirney, Inc. Flo-Mate 2000 (Frederick, MD). HOBO loggers (Onset Computer Corp., Bourne, MA) were installed within each PVC staff gauge and recorded temperature and atmospheric pressure in 10 minute intervals throughout the year-long monitoring from June 16, 2017 through June 15, 2018, resulting in approximately 52,000 data points per site across baseflow, storm flow, and other high flow conditions (e.g., snowmelt). An additional HOBO logger site was established on land near the approximate middle of our monitoring sites along Norris Creek near the intersection of Johnson and Pontaluna roads. Stage-pressure, stage-discharge, and pressure-discharge relationships were developed from site data and the

relationship with the highest R^2 value was used to create a stream hydrograph of each location (Appendix Table 1; Chu and Steinman 2009).

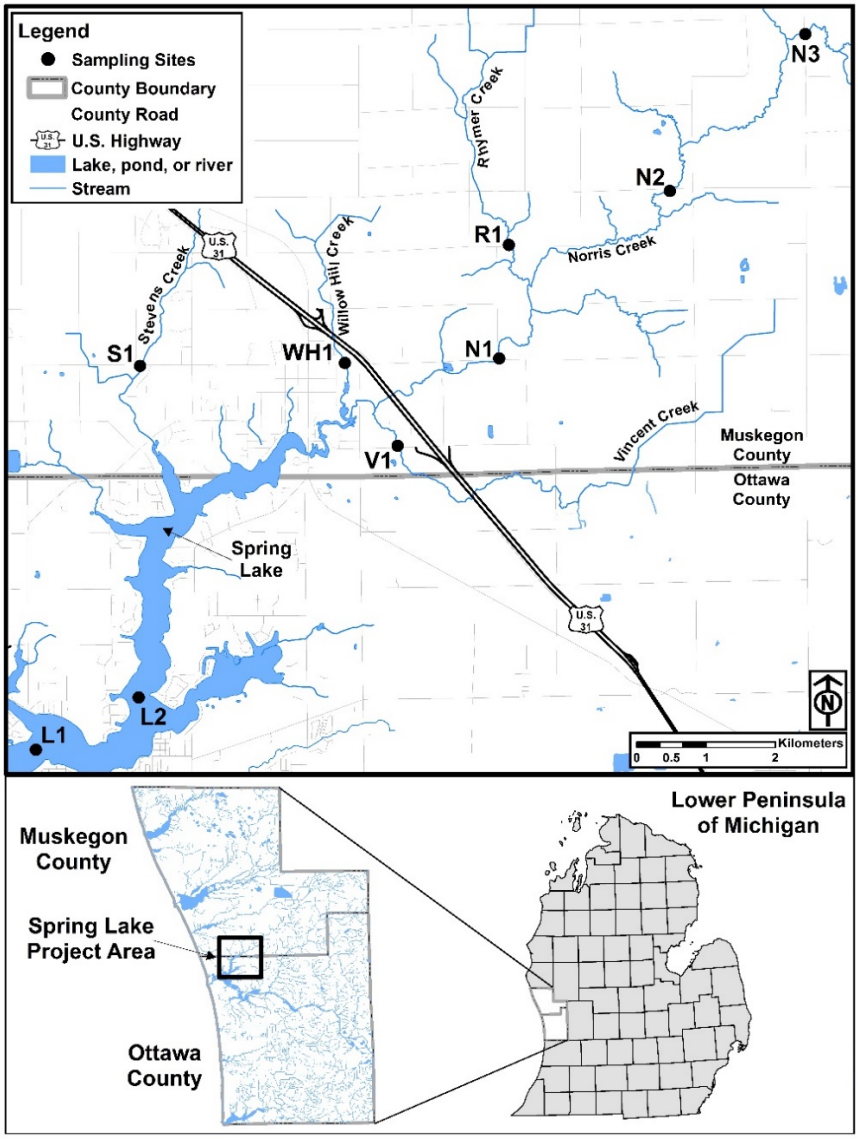

Figure 1. The Spring Lake watershed study area. Tributary sites are named after sampling locations (n = 7) and located on Stevens Creek, Willow Hill Creek, Rhymer Creek, Vincent Creek, and Norris Creek. Lake sites (L1, L2) are locations used in previous Spring Lake internal load studies (Steinman et al. 2018).

Surface water grab samples were collected in 1-L bottles, stored on ice, and returned to the lab for nutrient analysis, usually within 4 hours. General water quality parameters (dissolved oxygen [DO], temperature, pH, specific conductivity, total dissolved solids [TDS], redox potential [ORP: oxidation-reduction potential – the degree to which a substance is capable of oxidizing or reducing another substance], and turbidity) were measured in the field using a YSI 6600 (YSI, Inc., Yellow Springs, OH)

sonde. All water quality sample collections and measurements took place in the thalweg of the channel at the established stream transects.

In addition to tributary measurements, two sites (Fig. 1) were monitored in Spring Lake itself and sampled a total of four times on July 17, August 1, August 16, and August 30, 2017. These sites correspond to the two deeper sites we have sampled in the past. Sites were sampled at near-surface and near-bottom depths using a 1-meter vertical integrated sampler to collect water. The water was poured into a 10-L carboy gently inverted 10 times and subsampled into 1-L bottles and returned to the lab for nutrient analysis. General water quality parameters were measured at depth with a YSI 6600 sonde. Water for MC analysis was collected in amber glass jars and stored in a dark cooler at 4°C.

In the lab, water from each site was gently inverted and subsampled for analysis of P (soluble reactive P [SRP] and TP) and nitrogen (N) (ammonia [NH_3], nitrate [NO_3^-], and total Kjeldahl nitrogen [TKN]) species. Duplicate water quality samples and sonde measurements were taken every other month during baseflow conditions and all storm events. Water for SRP and NO_3^- analyses was syringe-filtered through acid-washed 0.45-µm membrane filters into scintillation vials; SRP was refrigerated at 4°C and NO_3^- was frozen until analysis. NH_3 and TKN were acidified with sulfuric acid and kept at 4°C until analysis. SRP, TP, NH_3, NO_3^-, and TKN were analyzed on a SEAL AQ2 discrete automated analyzer (U.S. EPA 1993). Any values below detection were calculated as ½ the detection limit.

MC toxin was measured using three methods: (1) using enzyme-linked immunosorbent assay (ELISA) tube kits to determine MC concentration, (2) high-performance liquid chromatography (HPLC) to determine total MC concentration along with three variants (MC-LR, MC-RR, and MC-YR), and (3) qPCR. Envirologix MC Tube Kits (Portland, ME) were used according to manufacturer instructions. The third method is still being validated so results from only methods 1 and 2 are reported.

HPLC was used to confirm the presence of MC and MC variants. Freeze-dried GF/F filters were extracted with 5% (*v/v*) acetic acid by ultra sonification for 5 min, then centrifuged at 10,000 RPM for 15 min at 4°C; the process was repeated three times. HLB cartridges (200 mg, Oasis®, Waters, MA, USA) were activated with 5 mL of methanol and 5 mL of distilled water, after which centrifuged supernatant was applied at a flow rate of 1 mL/min, washed again with 15 mL 5% (*v/v*) methanol, and a final elution with 10 mL 100% methanol. The eluent was dried under N_2 gas prior to reconstitution in 1.0 mL methanol

and a 500 µL sample was prepared for HPLC analysis. Quantification of MCs was performed on an Agilent 1200 series HPLC system with a DAD detector (Agilent, CA, USA) equipped with ODS column (Agilent Eclipse XDB-C18, 5 µm, 4.6 mm × 150 mm) as described by Su et al. (2015). Standards for MCs were obtained from Sigma-Aldrich (München, Germany). The concentration of total MC (TMC) is the sum of three MC variants, including MC-RR, MC-RR, and MC-YR (L, R, and Y are abbreviations of leucine, arginine, and tyrosine, respectively).

Data Analysis

Significant differences in water quality among sites across the year of sampling were conducted using one-way Analysis of Variance (ANOVA) tests, preceded by Shapiro-Wilk tests of normality and Brown-Forsythe tests for equal variance. Data that did not meet ANOVA test assumptions were transformed, or else analyzed via Kruskal-Wallis tests (one-way ANOVA on ranks). Post-hoc multiple comparison tests were conducted using either Holm-Sidak (following ANOVAs) or Dunn's test (following ANOVAs on ranks). All statistical tests were performed in SigmaPlot (v.14.0, Systat Software, Inc.).

Historical precipitation data logged in hourly increments at Muskegon County Airport across thirty years from 1988-2018 were downloaded from the National Oceanic and Atmospheric Administration's (NOAA) National Centers for Environmental Information (NCEI; formerly the National Climatic Data Center) local climate dataset and summed into days, months, and years as needed.

Hydrologic models were created using monthly stage measurements and atmospheric pressure time series data. For each site, stream atmospheric pressure sensor data were first corrected using the centralized HOBO logger data located in the center of the watershed on dry land near site R1. Next, atmospheric pressure and stage measurements were used to create a regression to calculate stage time series data. Discharge-stage and discharge-pressure models were created for each site and the better fitting model of the two was used in future analyses to model discharge. Hydrographs were created for modeled discharge at each site throughout the 2017-2018 monitoring period and were used alongside NCEI precipitation records to characterize storm events. During discharge model creation, site V1 (only) was found to have a stage-linked relationship that emerged as two separate patterns of data, roughly separated at the 40 cm stage mark. Two separate discharge models were created based on these patterns, with "V1 high" as the model built from stage data above 40 cm and "V1 low" from the stage data less than 40 cm.

The calculation method for hydraulic retention time (HRT) was modified from Lauber (1999). The June 2017 – June 2018 monitoring year was divided into time intervals, such that start or end dates of one interval were the median dates between two fieldwork baseflow sampling events. HRT was generally calculated for each time interval, by season (winter = 7 months [October-April]; summer = 5 months [May-September]), and for the entire monitoring year by using the formula below:

$$HRT\ (Y)\ = \frac{lake\ volume\ (AF)}{[stream\ discharge\ (AF/Y) + precipitation(AF/Y)]}$$

where Y = year and AF = acre-feet. Discharge data from the four most downstream sites in their respective tributaries (S1, WH1, V1, N1) were summed by sampling interval time and site prior to seasonal and annual HRT calculations.

Lake volume for the numerator of the HRT calculation was not directly measured during this study, so three values were selected to provide a range of potential values. Volumes from previous Spring Lake monitoring (Lauber 1999; Groves, pers. comm.) were referenced as known historical lake volumes. Data from NOAA's Great Lakes Environmental Research Laboratory's (GLERL) Great Lakes Dashboard (https://www.glerl.noaa.gov/data/dashboard/GLD_HTML5.html) was referenced to calculate annual mean water level of Lakes Michigan and Huron during this study, as well as Lauber's and Groves' sampling years, in order to create a proxy value for annual Spring Lake volume during 2017-2018 monitoring.

To calculate the denominator terms for HRT, stream discharge was calculated as the sum of baseflow (as measured in the field and generalized over each sampling interval) plus modeled storm flow volumes (calculated as modeled baseflow during sampling intervals subtracted from total modeled flow on hydrographs) from the sampled tributaries. This approach likely results in an underestimate of discharge reaching the lake because it does not account for runoff from impervious surfaces and unsampled outlets entering the lake. However, we anticipate that the tributary discharge accounts for the vast majority of inflows to Spring Lake. The comparison with the previous HRT calculation method for the Spring Lake watershed (Lauber 1999) is imperfect, as the methodology used by Lauber was not explicit.

P and N loads were calculated by multiplying nutrient concentrations with field-measured stream flow from each site and sampling date using the following formula and statistically summarized using the methods listed above.

$$Load\ \left(\frac{mg}{s}\right) = Concentration\ \left(\frac{mg}{L}\right) * Flow\ \left(\frac{m^3}{s}\right) * \left(\frac{1000\ L}{m^3}\right)$$

Finally, an annual P budget for Spring Lake was updated for the 2017-2018 monitoring year. Spring Lake internal P loading rates were previously reported by Steinman et al. (2018). Tributary loading rates were determined using data from this study by multiplying the seasonal TP mean or weighted annual TP mean with the corresponding seasonal or annual discharge and applying conversion rates as needed. Atmospheric deposition P rates were calculated based on a study of Silver Lake in Oceana County, MI, ~43 miles north of Spring Lake (Brennan et al. 2015). Septage, waterfowl, and stormwater runoff P loading rates were referenced from a previous Spring Lake monitoring study (Lauber 1999).

Results

Tributary Water Quality

In general, tributary water quality was good, with mean DO concentrations exceeding 10 mg/L during baseflow and declining to between 8-9.5 mg/L during storm events (Table 2). DO values less than 5 mg/L are indicative of impaired water quality.

Specific conductivity reflects the amount of ionized salts in solution. As chloride (Cl) is often one of the most common salts, there is usually a strong positive relationship between specific conductance and Cl. Conductivity is also used as an indicator of human disturbance in aquatic systems, as it tends to increase with increasing amount of urban development. In west Michigan, specific conductance generally ranges from 100 (precipitation and surface water-driven) to 600 µS/cm (more groundwater-dominated systems), with values > 600 suggesting human-induced stress to aquatic systems. Mean specific conductivity in the sampled Spring Lake tributaries during baseflow was well below 600, and dropped even farther during storm events (Table 2), suggesting dilution by stormwater runoff.

TDS is the portion of solids in water that can pass through a 2-µm filter. TDS is generally not considered a primary pollutant (i.e., it is not associated with health effects), but rather is used as an indication of aesthetic characteristics of drinking water and as an indicator of the presence of a broad array of chemical contaminants. Waters with high TDS levels are generally of inferior quality. In drinking water,

a limit of 0.5 g/L is desirable; Illinois has set a general water quality standard of 1.0 g/L for TDS. Mean TDS values were uniformly low (≤0.3 g/L) in our sampled tributaries (Table 2).

Turbidity indicates how "cloudy" the water is, and perhaps not surprisingly, mean turbidity values increased ~7-fold during storm events, as the runoff carries more particles in the water column after rain events.

Table 2. Mean (±SE) general water quality parameters at Spring Lake watershed monitoring sites. Data are divided into baseflow and storm flow (gray shading) by site. Storm sampling (~≥ 0.25 inches of rain proceeded by 72 hours of dry weather) occurred on 4 dates: 8/17/2017, 2/20/2018, 5/3/2018, and 5/31/2018.

Flow	Site	n	Temp (°C)	DO (mg/L)	SpCond (µS/cm)	TDS (g/L)	Turbidity (NTU)
Base	S1	12	9.02 (1.16)	10.40 (0.30)	346 (8)	0.225 (0.005)	3.0 (0.9)
	WH1	12	8.51 (1.85)	11.13 (0.48)	471 (18)	0.306 (0.012)	4.2 (0.6)
	V1	11	8.71 (2.20)	10.03 (1.03)	347 (16)	0.225 (0.010)	5.9 (2.9)
	N1	11	9.24 (2.15)	11.25 (0.60)	308 (8)	0.200 (0.005)	3.1 (0.7)
	R1	12	8.94 (1.98)	11.38 (0.53)	312 (9)	0.203 (0.006)	4.6 (0.6)
	N2	11	9.50 (1.96)	11.31 (0.55)	319 (9)	0.207 (0.006)	3.4 (1.0)
	N3	12	9.45 (1.69)	10.61 (0.45)	395 (14)	0.257 (0.009)	2.5 (0.3)
Storm	S1	4	12.19 (3.64)	9.26 (0.99)	300 (10)	0.195 (0.007)	24.9 (5.5)
	WH1	4	13.27 (4.04)	8.87 (1.13)	285 (40)	0.185 (0.026)	30.2 (3.8)
	V1	4	13.31 (4.34)	8.53 (1.46)	312 (21)	0.202 (0.014)	16.9 (5.7)
	N1	4	14.13 (3.87)	9.12 (1.09)	251 (18)	0.163 (0.011)	32.3 (3.0)
	R1	4	13.26 (3.75)	9.33 (0.96)	250 (24)	0.163 (0.015)	22.2 (3.3)
	N2	4	13.59 (3.27)	9.18 (0.78)	238 (14)	0.154 (0.009)	21.8 (10.7)
	N3	4	12.86 (3.03)	8.94 (0.76)	318 (21)	0.207 (0.014)	16.1 (11.4)

SRP concentrations were relatively low during baseflow, and changed little during storm events (Table 3). The upstream Norris Creek site (N3) had significantly higher SRP concentrations than a number of other sites during baseflow and was higher than all other sites during storm flow (Table 4), but the absolute difference in concentration was modest. On average, SRP contributed 30 to 42% of the TP concentration during baseflow but only 9 to 15% of TP during storm flow (Table 3).

Mean TP concentrations ranged from 15 to 35 µg/L during baseflow but increased ~4-fold, from 65 to 125 µg/L, during storm flow (Table 3). Among sites, N3 again had significantly higher TP concentrations than WH1 or V1 (Table 4) but there were no significant differences during storm flow on account of the higher variability (Tables 3, 4).

There was an interesting temporal change in both SRP and TP concentrations, with substantial increases especially for SRP on the last two baseflow sampling dates at all sites, but most noticeably at N3 (Fig. 2); this site is the most upstream location along Norris Creek and is the closest site to the agricultural area of the watershed. This increase in P may be due to spring fertilizer application in the watershed, although the actual source(s) is not known.

Although the major focus in Spring Lake has been on P, there is concern that because of excess P enrichment, N is becoming a secondarily limiting nutrient (cf. Kramer et al. 2018) for phytoplankton growth. As a consequence, we also measured various N species. However, all three forms of N: nitrate (NO_3^-), ammonia (NH_3), and total Kjeldahl nitrogen (TKN), were relatively low in concentration, and storm flow elevated concentrations either minimally (nitrate) or no more than two-fold (NH_3 and TKN; Table 3). The spring increase observed for P was not evident for the N species (Fig. 2). Nitrate did spike at R1 only during November and May baseflow and NH_3 concentrations were not in synchrony among tributaries over time (Fig. 3).

Table 3. Mean (±SE) nutrient concentrations at Spring Lake watershed monitoring sites. Data are divided into baseflow and storm flow by site.

Flow	Site	n	SRP (µg/L)	TP (µg/L)	NO_3^- (mg/L)	NH_3 (mg/L)	TKN (mg/L)
Base	S1	12	9 (1)	23 (3)	0.73 (0.03)	0.03 (0.01)	0.42 (0.03)
	WH1	12	6 (1)	15 (3)	0.45 (0.06)	0.04 (0.01)	0.45 (0.02)
	V1	11	8 (1)	22 (4)	0.47 (0.08)	0.05 (0.01)	0.48 (0.02)
	N1	11	9 (1)	23 (3)	0.73 (0.12)	0.02 (0.01)	0.47 (0.04)
	R1	12	7 (1)	23 (3)	1.34 (0.37)	0.04 (0.01)	0.56 (0.05)
	N2	11	11 (1)	26 (3)	0.62 (0.07)	0.03 (0.01)	0.45 (0.03)
	N3	12	14 (1)	35 (3)	0.97 (0.13)	0.06 (0.01)	0.63 (0.05)
Storm	S1	4	9 (1)	77 (6)	0.73 (0.12)	0.07 (0.02)	1.13 (0.17)
	WH1	4	7 (1)	65 (6)	0.38 (0.06)	0.10 (0.02)	0.98 (0.14)
	V1	4	7 (1)	66 (20)	0.40 (0.06)	0.10 (0.02)	0.90 (0.14)
	N1	4	10 (0)	95 (18)	0.60 (0.05)	0.08 (0.02)	0.92 (0.15)
	R1	4	8 (1)	90 (7)	0.74 (0.09)	0.07 (0.01)	1.11 (0.11)
	N2	4	11 (2)	100 (25)	0.46 (0.03)	0.07 (0.02)	1.06 (0.20)
	N3	4	19 (3)	125 (75)	0.91 (0.18)	0.12 (0.06)	0.96 (0.31)

Table 4. Statistical analysis results comparing nutrient concentrations across sites using 1-way ANOVAs (normally distributed data) or Kruskal-Wallis (KW) 1-way ANOVA on ranks (non-normally distributed data). Data marked NS are not significantly different across sites. Tests marked with * had data square-root transformed prior to analysis.

	Baseflow			Storm Flow		
Parameter	Test	P	Post-Hoc Result	Test	P	Post-Hoc Result
SRP	KW	<0.001	N3 > WH1; p < 0.001 N3 > R1; p = 0.001 N3 > V1; p = 0.031 N2 > WH1; p = 0.002	ANOVA	<0.001	N3 > V1; p < 0.001 N3 > WH1; p < 0.001 N3 > R1; p < 0.001 N3 > S1; p = 0.001 N3 > N1; p = 0.003 N3 > N2; p = 0.015
TP	KW	<0.001	N3 > WH1; p < 0.001 N3 > V1; p = 0.049	KW	0.319	NS
NO_3^-	KW	<0.001	R1 > WH1; p < 0.001 R1 > V1; p = 0.011 N3 > WH1; p = 0.004 N3 > V1; p = 0.039 S1 > WH1; p = 0.029	ANOVA*	0.003	N3 > WH1; p = 0.013 N3 > V1; p = 0.019
NH_3	KW	0.224	NS	KW	0.762	NS
TKN	KW	0.041	N3 > S1; p = 0.025	KW	0.676	NS

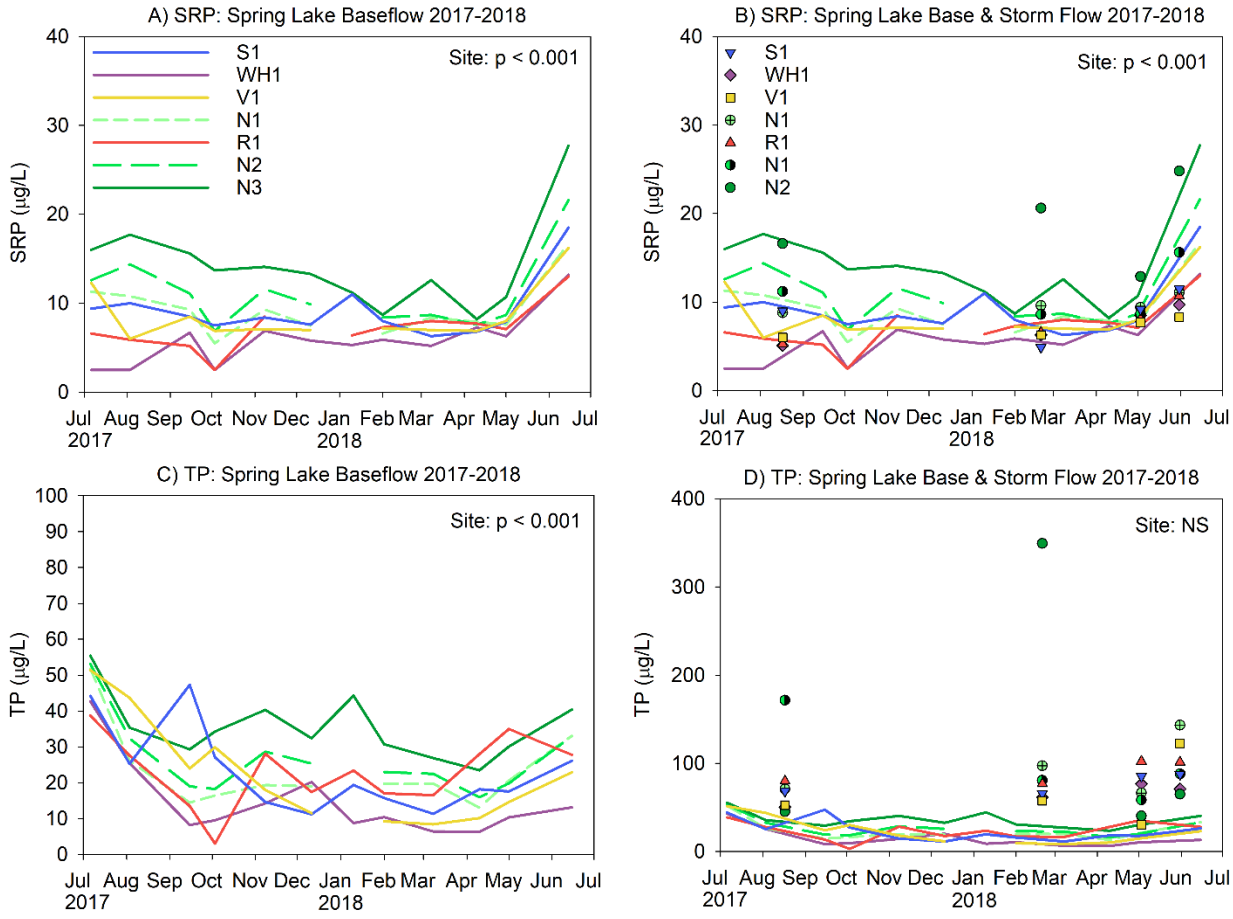

Figure 2. Soluble reactive phosphorus (SRP) (A, B) and total phosphorus (TP) (C, D) concentrations measured at the Spring Lake watershed monitoring sites in 2017-2018. Colored TP baseflow lines in D are magnified in C, which allow us to include both baseflow and storm event concentrations in D; symbols represent storm events. Legends in A, B applies to C, D.

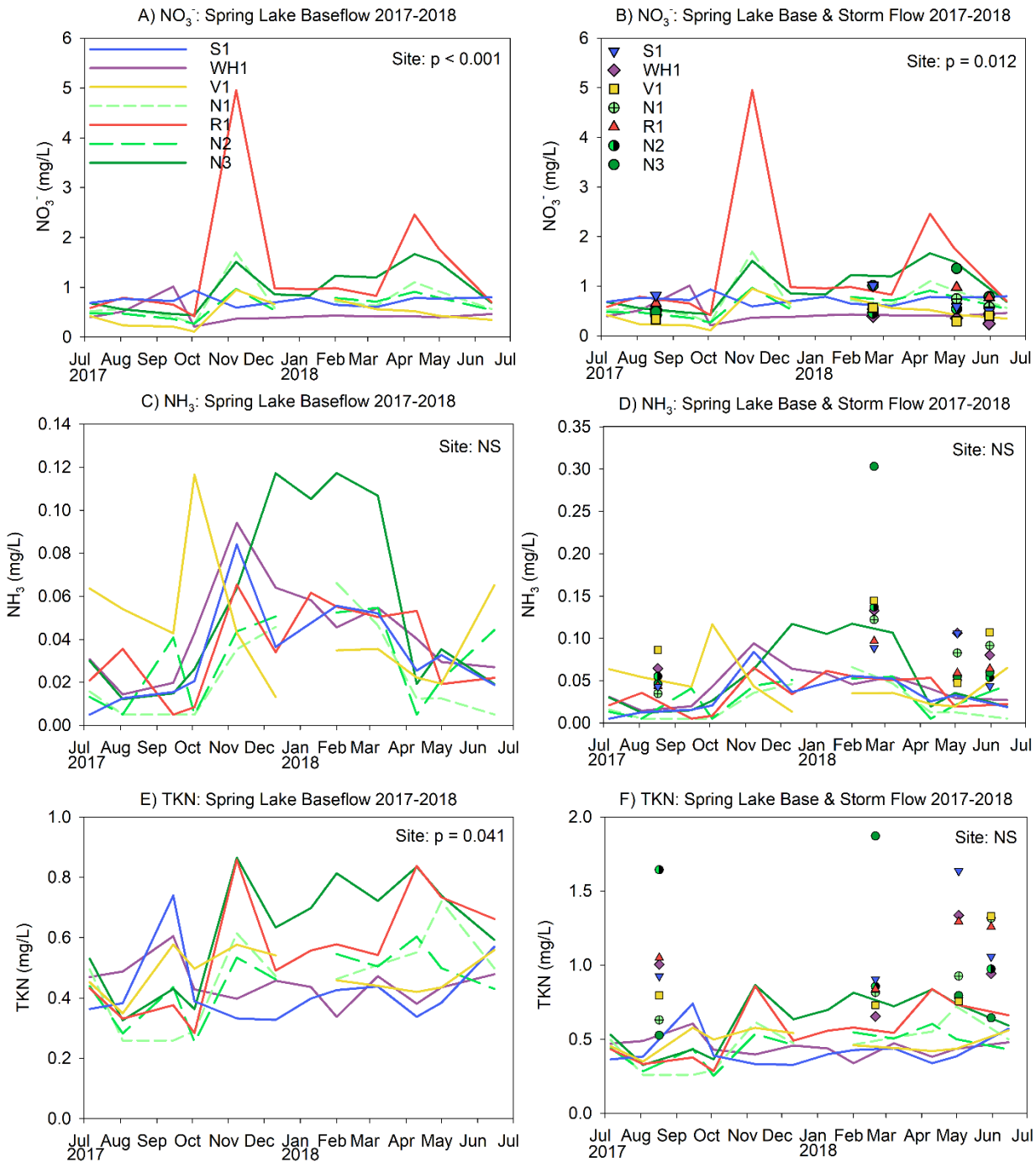

Figure 3. Nitrate (NO_3^-) (A, B), ammonia (NH_3) (C, D), and total Kjeldahl nitrogen (TKN) (E, F) concentrations measured at Spring Lake watershed monitoring sites in 2017-2018. Colored data lines in D and F are magnified in C and E, which allow us to include both baseflow and storm event concentrations in same graph; symbols represent storm events. Legend in A, B applies to other panels.

Hydrologic Characteristics

Precipitation during our sampling campaign (June 2017-June 2018) was greater than both the long-term (30 yr) median in most months (Fig. 4) and 1997-1998 when Lauber (1999) previously calculated a HRT for Spring Lake. Actual monthly precipitation values for each year are provided in Appendix Table 2. The wetter-than-average year has implications for the HRT calculation (see below).

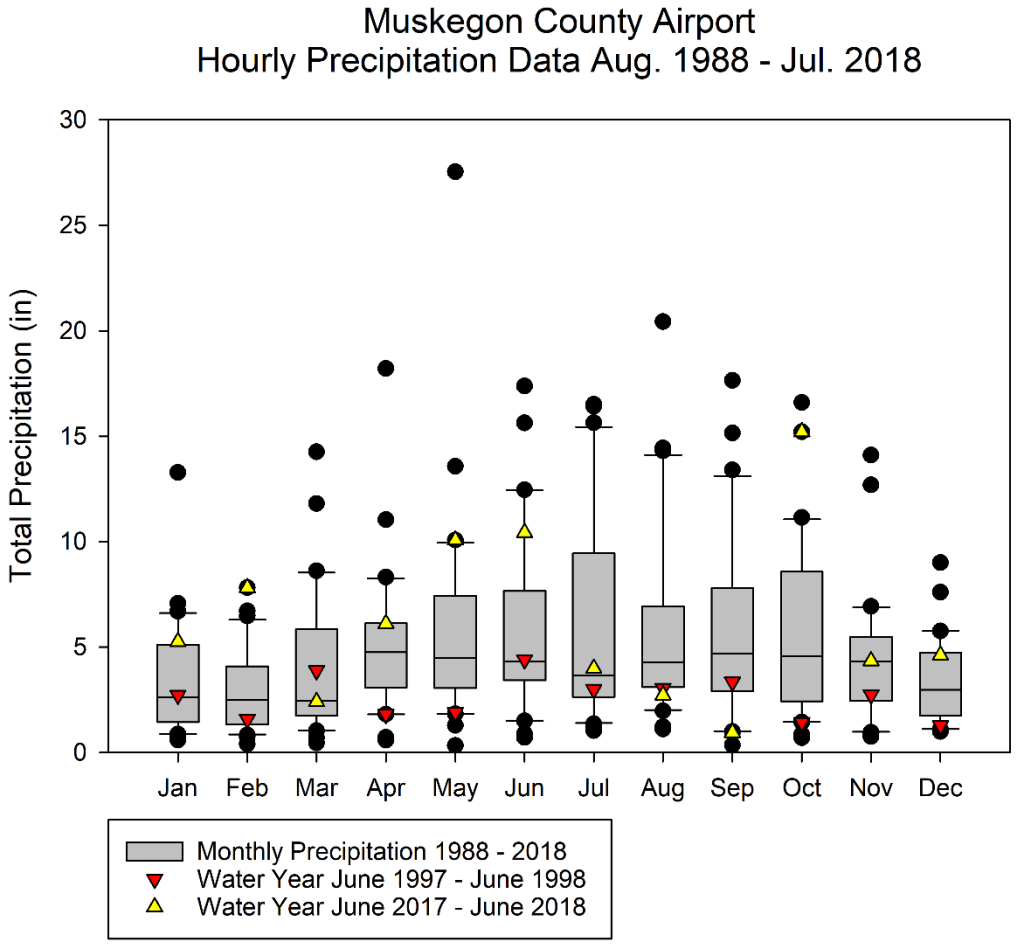

Figure 4. Muskegon County Airport precipitation records over thirty years from 1988-2018. Hourly precipitation records were downloaded during August 2018 from NCEI local climate dataset and summed into months (each month's box and whisker plot contains data across n = 30 years). Black circles are statistical outlier years in monitoring history for that month. "Water Year" represents a June 16 – June 15 (365 days total) time frame, to coincide with AWRI's 2017-2018 Spring Lake tributary monitoring. A water year with equal dates from 1997-1998 represents precipitation during a previous Spring Lake tributary monitoring study (Lauber 1999). The half-Junes per each water year are summed for this figure to be comparable to historic calendar year data.

Stream hydrographs were generated for each site (Appendix Figs. 1-8); the two hydrographs presented in Figs. 5 and 6 demonstrate that the majority of flow at downstream Norris Creek site N1 appears to originate in the Rhymer Creek R1 tributary, not upstream in Norris Creek (i.e., sites N2 or N3), given the similar peaks (albeit, as expected, the discharge at R1 is lower than at N1).

A) Norris Creek station N1, located at Pontaluna Road.

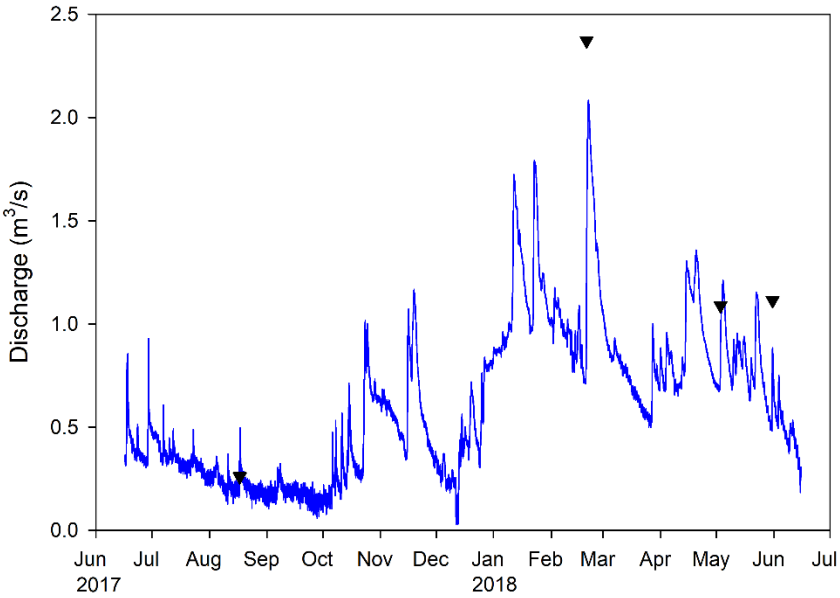

B) Rhymer Creek station R1, located at Mount Garfield Road.

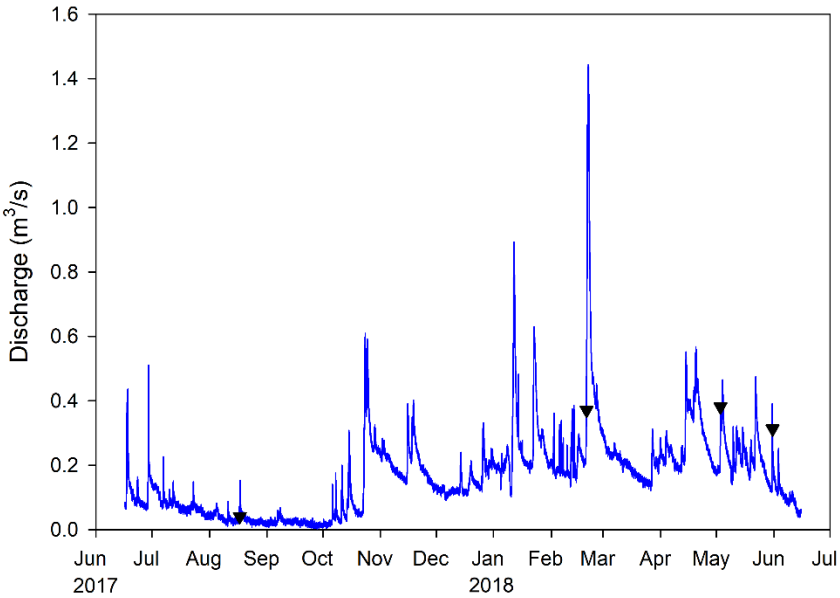

Figure 5. Example hydrograph models for A) N1 and B) R1 sites from June 16, 2017 – June 15, 2018. Inverted triangles indicate *in situ* storm sampling events. Note lower y-axis scale in R1 panel.

A May 3, 2018 storm hydrograph reveals that it takes about 24 to 36 hr after peak rainfall for peak discharge to occur (Fig. 6). Stevens Creek and Willow Hill Creek responded the quickest but their overall discharge was very low compared to the other sampling sites (Fig. 6). The Norris Creek sites responded the slowest to peak discharge but they also had the greatest flow.

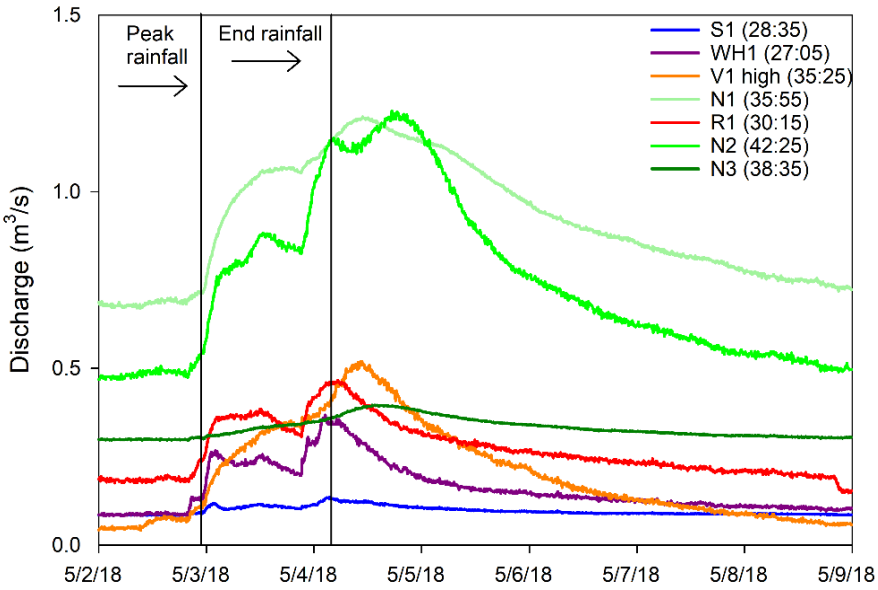

Figure 6. Overlaid storm hydrographs from all tributary sites during 5/3/18 storm event. Time between peak rainfall and peak discharge per site (hh:mm) is provided in the legend.

A hydrologic summary of the 5 major storms during the sampling year is presented in Table 6. The amount of rainfall varied 8-fold across storms, storm duration ranged 10-fold across storms, and intensity varied ~2-fold across storms (Table 6). The lower Norris Creek sites (N1 and N2) had the highest baseflow and storm event discharges.

Table 6. Hydrologic summary data, including storm event information. Rainfall, duration, and intensity are given for each storm sampling event and are reported and/or calculated from NCEI hourly data from Muskegon County Airport. For each monitoring location, average discharge (Q) of all monthly baseflow events, average Q during each individual storm sampling event, and storm flow duration are summarized. Sites are presented in in sampling order, from downstream to upstream in the watershed.

			Storm/High Flow* Event				
		Baseflow	8/17/2017	10/23/2017*	2/20/2018	5/3/2018	5/31/2018
	Rainfall (in)	--	1.15	8.22	4.58	4.50	1.00
	Rainfall Duration (h)	--	10	58	36	40	4
	Intensity (in/h)	--	0.12	0.14	0.13	0.11	0.25
S1	Avg Q (m^3/s)	0.094	0.109	0.225	0.310	0.111	0.102
	Storm Q Duration (h)	--	14.67	139.83	65.83	58.83	6.50
WH1	Avg Q (m^3/s)	0.087	0.082	0.251	1.077	0.236	0.165
	Storm Q Duration (h)	--	16.17	137.83	71.33	60.50	24.83
V1 high	Avg Q (m^3/s)	0.060	0.062	0.659	0.602	0.283	0.141
	Storm Q Duration (h)	--	17.00	136.50	50.67	100.00	26.83
N1	Avg Q (m^3/s)	0.511	0.322	0.763	1.343	0.978	0.745
	Storm Q Duration (h)	--	35.67	124.83	306.83	127.50	30.50
R1	Avg Q (m^3/s)	0.115	0.069	0.350	0.891	0.367	0.240
	Storm Q Duration (h)	--	35.83	138.83	72.00	47.17	25.50
N2	Avg Q (m^3/s)	0.430	0.316	1.264	1.214	0.811	0.455
	Storm Q Duration (h)	--	42.00	143.17	306.67	129.83	25.83
N3	Avg Q (m^3/s)	0.193	0.130	0.266	ND	0.344	0.286
	Storm Q Duration (h)	--	16.50	139.83	0.00	111.83	21.83

*The rain event on 10/23/2017 did not meet storm flow sampling criteria; however, stream discharge was measured regardless due to the magnitude of rainfall in order to improve the hydrologic modeling dataset.

Although sediment is not considered to be a major impairment in Spring Lake, it can affect the biology of the tributaries. It is clear that turbidity can increase 5 to 10-fold during storm events, as the power of elevated storm discharge moves sediment from both surface soils and streambanks (Fig. 7).

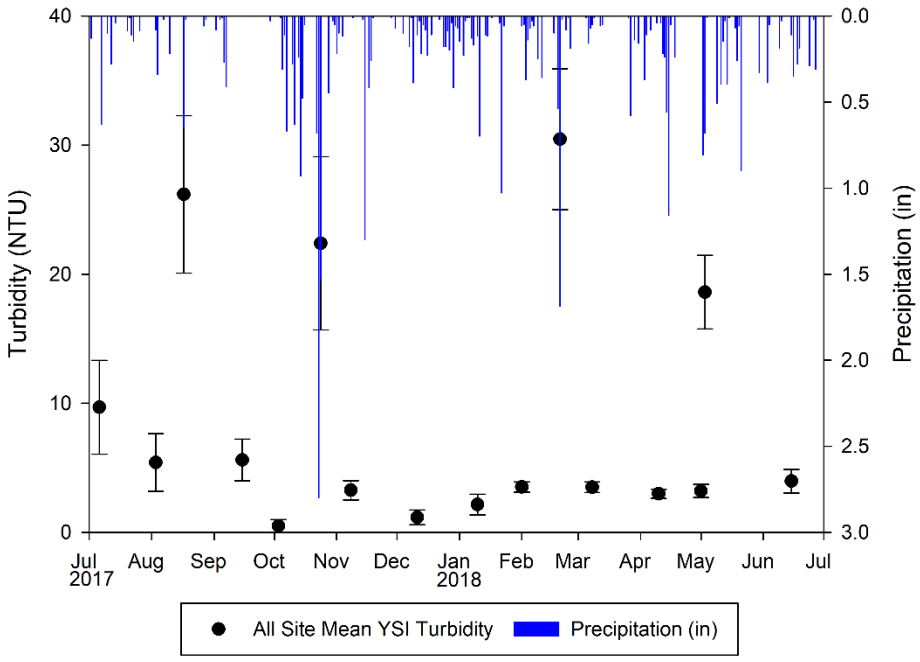

Figure 7. Daily precipitation and mean YSI turbidity (NTU) measurements from storm and monthly baseflow sampling events and a high flow event (10/24/2017; didn't meet our criteria as a storm event due to precipitation within 72 hr of big storm flow) during 2017-2018 sampling year. Hourly precipitation data were retrieved from the National Oceanographic and Atmospheric Administration's National Centers for Environmental Information (NOAA-NCEI) website and summed into days.

To calculate HRT for Spring Lake, we applied three different estimates for Spring Lake volume to try and capture the range of uncertainty in this measurement. The Lauber and GLERL volumes were very similar, and hence their annual HRT are identical for both approaches, although both are about 20% longer than the volume estimate from of Groves (12 vs. 15.5 months, respectively; Table 7). As one would expect, the HRT is shorter in winter when conditions tend to be wetter overall than in summer (Table 7).

Table 7. Hydraulic retention time (HRT) estimates for 2017-2018 sampling year, using Spring Lake volumes from Lauber (1999) and Tony Groves (2014). NOAA-GLERL volume based on Lakes Michigan-Huron water levels from 2017-2018 sampling months. Discharge (Q) is the total sum of precipitation, modeled, and field-measured flow in acre-feet volumes as described in each HRT calculation approach. Seasonal HRT calculations incorporate the total Q from all sampling intervals within each seasonal boundary; HRT (months) multiply that result based on the number of months per season (summer n=5; winter n=7). Annual mean HRT is a weighted average based on the number of days per each season (summer n=157; winter n=208) as determined by sampling intervals; mean HRT (months) multiplies the weighted mean (year) by 12 to convert to units of months.

	HRT Calculation	[lake pptn + modeled storm flow + field baseflow]		
	Source: (lake volume in acre-feet [af])	Lauber 1997-98 (25,132)	Groves 2014 (19,845)	GLERL proxy 2017-18 (25,108)
Summer (May-Sep)	Q (af/season)	12,307		
	HRT (season)	2.04	1.61	2.04
	HRT (months)	10.21	8.06	10.20
Winter (Oct-Apr)	Q (af/season)	34,378		
	HRT (season)	0.73	0.58	0.73
	HRT (months)	5.12	4.04	5.11
Annual (12 months)	Q (af/year)	46,685		
	Mean HRT (year)	1.29	1.02	1.29
	Mean HRT (months)	15.54	12.27	15.53

Load Data

The highest nutrient loads (both P and N) were measured in N1 (Table 8). Load is calculated as discharge × concentration; in the case of N1, both concentration and discharge were greater than the other sites (Tables 3 and 8, respectively), but the disparity among sites was much larger in discharge than in concentration. While nutrient loads at N1 were greater than other sites during both baseflow and storm events, they were statistically significant only during baseflow (Table 9), presumably because of greater variation during storms. Overall, storm flow had a much greater effect on TP, NH_3 and TKN loads than either SRP or NO_3^- loads (Table 8).

Table 8. Mean (±SE) nutrient loads at Spring Lake watershed monitoring sites, based on field-measured discharge during sampling events. Data are divided into baseflow and storm flow (grey shading) by site.

Flow	Site	n	SRP (mg/s)	TP (mg/s)	NO_3^- (mg/s)	NH_3 (mg/s)	TKN (mg/s)
Base	S1	12	1 (0)	2 (0)	66 (7)	4 (1)	39 (5)
	WH1	12	1 (0)	1 (0)	38 (7)	5 (1)	39 (9)
	V1	11	1 (0)	2 (1)	116 (51)	6 (2)	89 (36)
	N1	11	5 (1)	13 (3)	479 (119)	21 (8)	307 (72)
	R1	12	1 (0)	3 (1)	195 (64)	5 (1)	76 (17)
	N2	11	3 (1)	8 (2)	229 (58)	14 (5)	164 (45)
	N3	12	3 (1)	7 (1)	200 (45)	15 (6)	130 (30)
Storm	S1	4	2 (0)	15 (3)	148 (51)	15 (6)	227 (64)
	WH1	4	2 (1)	17 (5)	86 (24)	26 (9)	244 (81)
	V1	3	2 (1)	19 (15)	75 (46)	18 (13)	231 (155)
	N1	4	12 (4)	120 (47)	716 (235)	123 (59)	1143 (377)
	R1	4	2 (1)	26 (8)	210 (71)	20 (7)	310 (97)
	N2	4	7 (2)	58 (18)	292 (108)	62 (40)	617 (182)
	N3	4	8 (5)	102 (94)	400 (244)	90 (81)	600 (488)

Table 9. Statistical analysis results comparing nutrient loads across sites using 1-way ANOVAs (normally distributed data) or Kruskal-Wallis 1-way ANOVA on ranks (non-normally distributed data). Data marked NS are not significantly different across sites.

	Baseflow			Storm Flow		
Parameter	Test	P	Post-Hoc Result	Test	P	Post-Hoc Result
SRP	KW	<0.001	N1 > WH1; p < 0.001 N1 > R1; p = 0.007 N1 > V1; p = 0.012 N1 > S1; p = 0.012 N3 > WH1; p = 0.004 N2 > WH1; p = 0.006	KW	0.028	NS
TP	KW	<0.001	N1 > WH1; p < 0.001 N1 > S1; p = 0.014 N1 > V1; p = 0.021 N3 > WH1; p = 0.005 N2 > WH1; p = 0.010	KW	0.177	NS
NO3	KW	0.002	N1 > WH1; p = 0.003 N1 > V1; p = 0.041	KW	0.097	NS
NH3	KW	0.536	NS	KW	0.627	NS
TKN	KW	0.003	N1 > WH1; p = 0.010 N1 > S1; p = 0.048	KW	0.292	NS

Overall, SRP and TP loads were greatest in Norris Creek; during baseflow, loads tended to be higher in winter, especially in December, than in summer (Fig. 8). However, the absolute difference in loads during baseflow is relatively minor, as is evident when storm loads are compared with baseflow loads (Fig. 8d). Hence, although episodic, most of the TP load to Spring Lake likely comes during just a few major storm events during the year. Baseflow accounts for more of the annual SRP and N loads compared to TP (Figs. 8, 9), but again, most of these nutrient loads come during storm events.

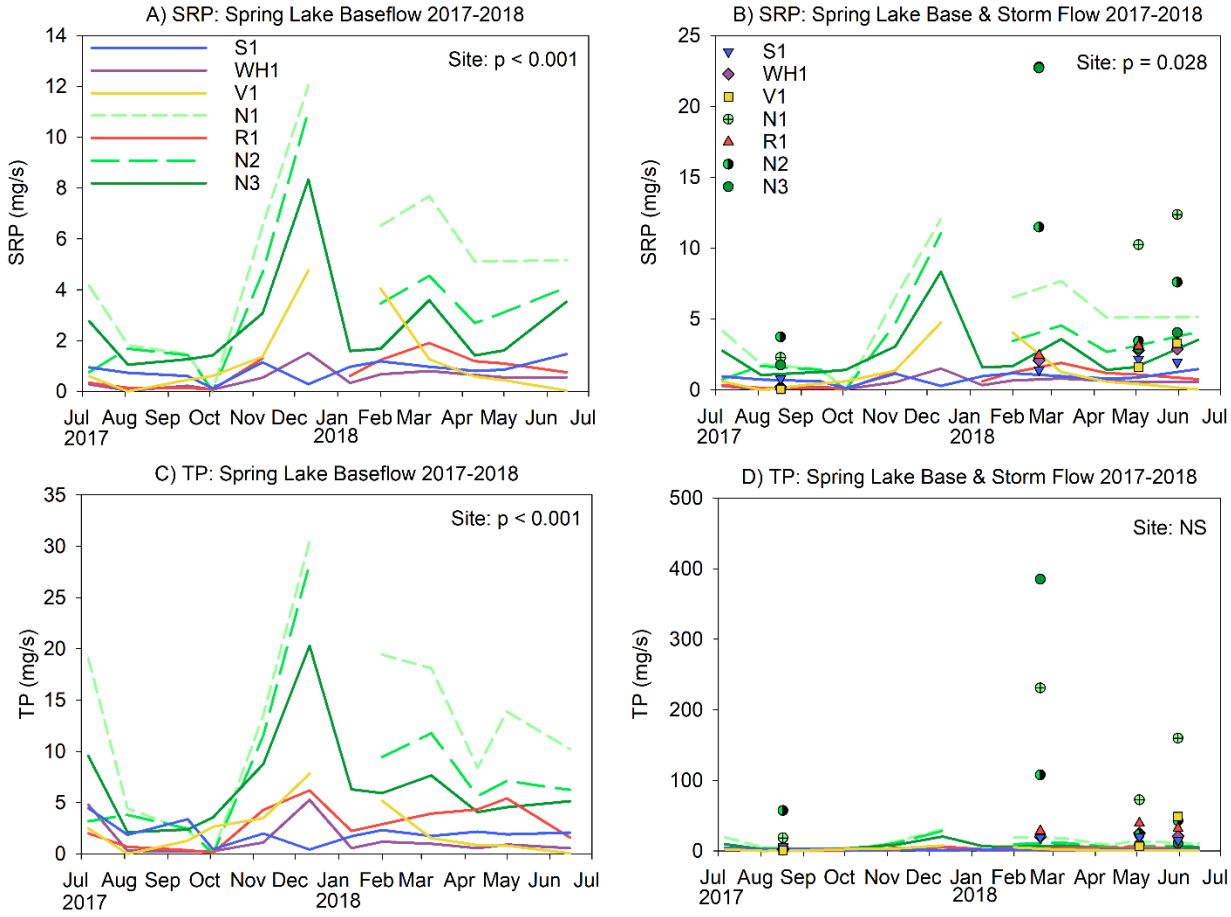

Figure 8. Soluble reactive phosphorus (SRP) (A, B) and total phosphorus (TP) (C, D) loads measured at Spring Lake watershed monitoring sites in 2017-2018. Colored data lines represent the baseflow data; lines in C are minimized in D, which allow us to include both baseflow and storm event concentrations in same graph; symbols represent storm events. Legend in A, C also applies to B, D. No load data for January due to ice cover precluding discharge measurements.

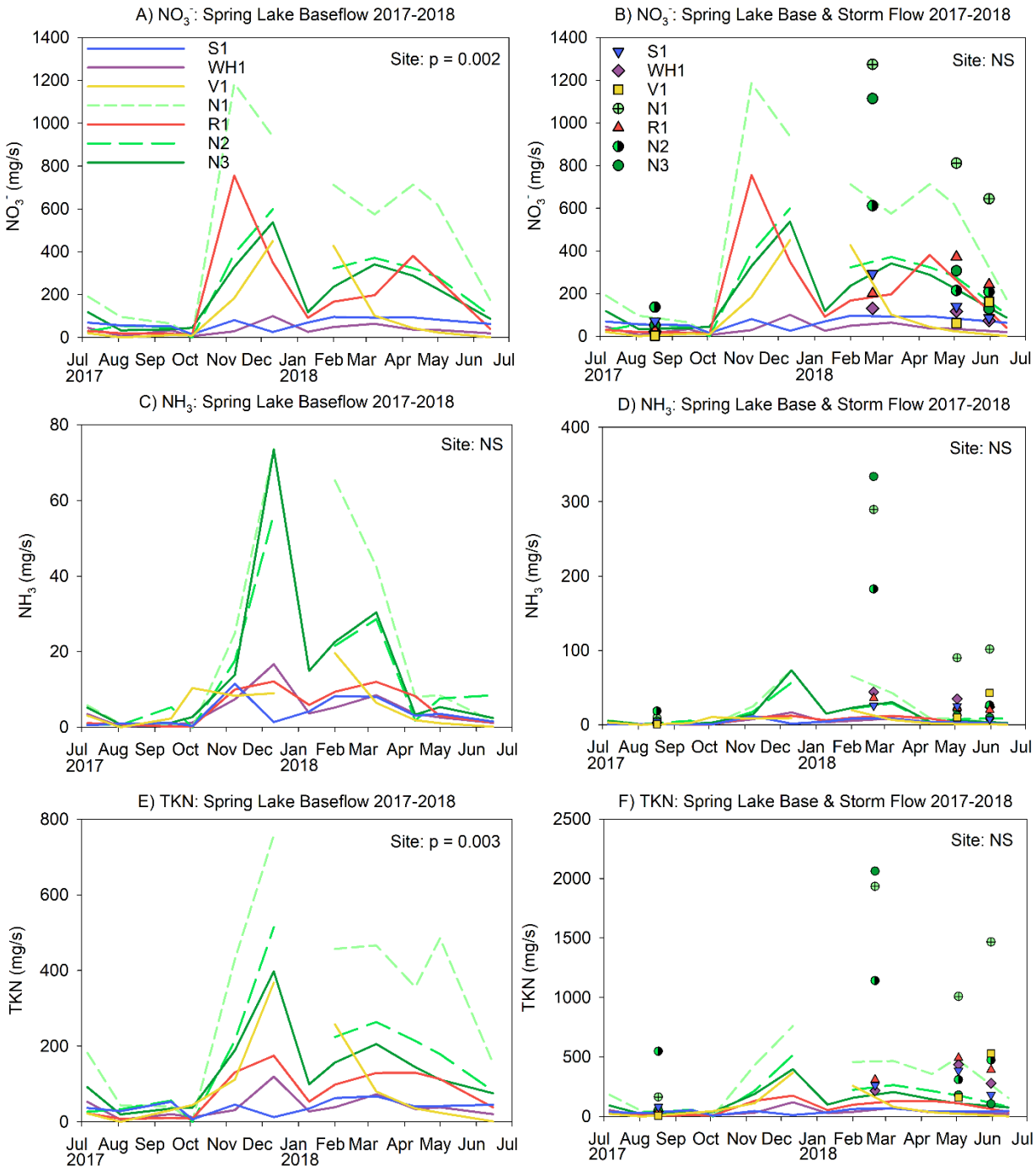

Figure 9. Nitrate (NO_3^-) (A, B), ammonia (NH_3) (C, D), and total Kjeldahl nitrogen (TKN) (E, F) loads measured at Spring Lake watershed monitoring sites in 2017-2018. Colored data lines represent the baseflow data; lines in C and E are minimized in D and F, respectively, which allow us to include both baseflow and storm event concentrations in same graph; symbols represent storm events. Legend in A applies to D and E; legend in B applies to D and F. No load data for January due to ice cover precluding discharge measurements.

Our P budget (Table 10) reveals that external loading accounts for about 70% of the total P load reaching Spring Lake based on our estimates, and tributary loading accounts for most (~65%) of that external load. However, the budget includes several external sources from Lauber's thesis (1999) that are likely no longer correct due to changes in the watershed. For example, the septage and lawn fertilizer estimates are likely lower in 2018 than in 1999 due to extension of sewer systems and a reduction in P fertilizer applications. The actual magnitude of these reductions was beyond the scope of this study, but certainly needs to be updated. Each of these sources has considerable uncertainty associated with them, which is discussed in more detail in the Discussion.

Table 11 provides details on the tributary loading calculations in Table 10. First, site average TP was calculated by taking the seasonal mean or weighted annual mean for each the four downstream sites (S1, WH1, V1, N1), and then deriving a grand mean site average. Next, discharge (Q) was taken from the previously summarized HRT calculation (Table 7). Tributary load values were calculated by multiplying site average TP and Q, then applying appropriate conversion factors.

Table 10. Spring Lake annual P budget.

Data	Source	Reference	Mean Annual P (kg)	Mean Annual P (%)
internal loading	Steinman el al. 2017	p.18	1,007[a]	28.6
tributary loading	this report		1,621[b]	46.0
atmospheric deposition	Brennan et al. 2015	p.24	76[c]	2.2
septage	Lauber 1999	p.67; 177	491[d]	13.9
waterfowl	Lauber 1999	p.67; 175	16[e]	0.5
lawn fertilizer	Lauber 1999		267	7.6
shoreland runoff	US EPA 1996	Lauber p.159	48[f]	1.4
TOTAL			3,526	100.2

[a]Mean of TP release rates under anoxic conditions, assuming constant rates for ½ of year (Steinman et al. 2009), over entire lake surface area

[b]Based on load calculations from this study

[c]Based on atmospheric deposition data from Silver Lake, MI (Brennan et al. 2015) and Lauber (1999) Spring Lake surface area

[d]From Lauber thesis

[e]From Lauber thesis

[f]Based on USEPA (1996) value of 0.5 mg/L mean TP in storm water from all land use types multiplied by runoff discharge, which was calculated by precipitation in Lauber (1999) multiplied by surface area within 500ft of shoreline.

Table 11. Summary data used to derive tributary loading calculation in Table 10.

	Site Avg TP (mg/L)	Q (af/season or year)	Tributary Loading (kg TP)
Summer (May-Sep)	0.0282	12,307	427
Winter (Oct-Apr)	0.0150	34,378	1,194
Annual (12 months)	0.0207	46,685	1,621

Lake Data

The water quality data at the two sampling sites were consistent with prior studies. In mid-summer at sites with greater depth, there is often evidence of depleted oxygen concentrations (hypoxia to anoxia), although water temperatures showed weak evidence of stratification (Table 12). Mean SRP concentrations were elevated at the near-bottom compared to the surface although that was not the case for TP (Table 13, Fig. 10). This is in contrast to 2016, when bottom TP concentrations at deeper sites were above 300 at one site and close to 1,000 µg/L at another (Steinman et al. 2018). This difference may be related to a later sampling date in 2016 (12 September) than in 2017 (mid-July through the end of August). The low DO concentrations likely accounted for the greater ammonia concentrations at depth, as well (Table 13, Fig. 11).

Chlorophyll concentrations at both sites were quite high (Table 14, Fig. 12). MC concentrations were somewhat greater when measured with the more sensitive HPLC instrument than ELISA kits (Figs. 13, 14), but in both cases, total concentrations ranged from 0.1 to 6 µg/L. Using HPLC, the most abundant variant was MC-RR (Table 14, Fig. 14).

Table 12. Mean (±SE) general water quality parameters at Spring Lake monitoring sites. For each site, n=4 sampling dates (biweekly from mid-July to end of August, 2017).

Site	Depth	n	Temp (°C)	DO (mg/L)	SpCond (µS/cm)	TDS (g/L)	Turbidity (NTU)	Light Ext. (µmol/m^2/s)
Site 1	Top	4	24.87 (0.74)	10.33 (0.49)	520 (6)	0.338 (0.004)	9.4 (1.9)	1.6 (0.0)
	Bottom	4	21.04 (1.07)	2.33 (1.22)	577 (25)	0.375 (0.016)	16.7 (8.3)	
Site 2	Top	4	25.39 (0.70)	11.68 (0.62)	506 (7)	0.329 (0.004)	11.0 (2.8)	1.8 (0.0)
	Bottom	4	19.88 (1.13)	0.42 (0.06)	557 (8)	0.362 (0.005)	4.6 (0.2)	

Table 13. Mean (±SE) nutrient concentrations at Spring Lake monitoring sites. For each site, n=4 sampling dates.

Site	Depth	n	SRP (µg/L)	TP (µg/L)	NO_3^- (mg/L)	NH_3 (mg/L)	TKN (mg/L)
Site 1	Top	4	3 (1)	45 (10)	0.04 (0.03)	0.01 (0.00)	1.10 (0.06)
	Bottom	4	17 (15)	59 (22)	0.16 (0.05)	0.10 (0.07)	1.07 (0.03)
Site 2	Top	4	3 (1)	56 (10)	0.08 (0.03)	0.02 (0.00)	1.00 (0.05)
	Bottom	4	15 (6)	64 (5)	0.21 (0.03)	0.20 (0.06)	0.88 (0.07)

Table 14. Mean (±SE) chlorophyll *a* (Chl *a*) and microcystin (MC) at Spring Lake monitoring sites. For each site, n=4 sampling dates.

Site	Depth	n	Chl *a*, ext. (µg/L)	MC, ELISA (µg/L)	MC-RR (µg/L)	MC-YR (µg/L)	MC-LR (µg/L)	TMC (µg/L)
Site 1	Top	4	58.3 (7.4)	0.5 (0.5)	1.8 (0.8)	0.9 (0.2)	0.3 (0.2)	3.1 (1.0)
	Bottom	4	39.4 (4.6)	0.2 (0.2)	1.5 (0.2)	0.5 (0.1)	0.3 (0.2)	2.3 (0.3)
Site 2	Top	4	63.5 (8.5)	0.2 (0.1)	2.1 (0.5)	1.0 (0.2)	0.3 (0.2)	3.3 (0.6)
	Bottom	4	15.7 (4.6)	0.5 (0.3)	1.9 (0.4)	0.5 (0.2)	0.2 (0.1)	2.5 (0.5)

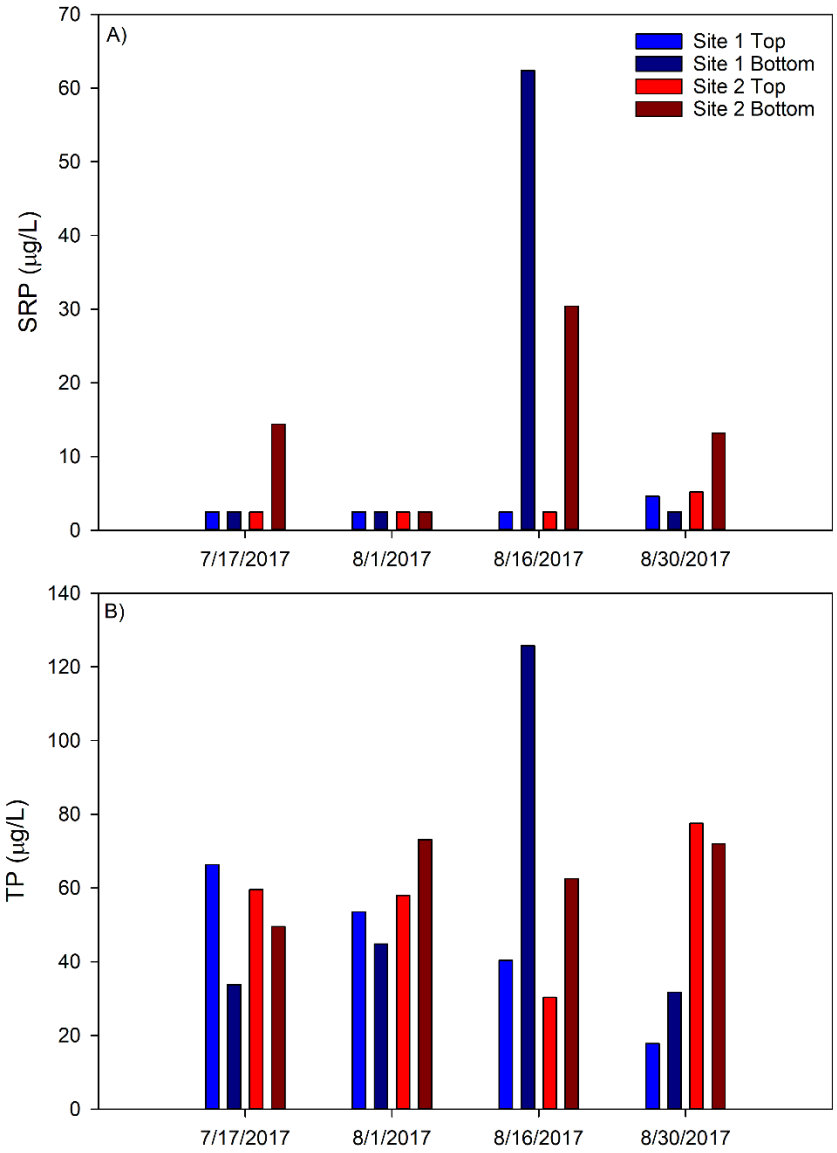

Figure 10. Soluble reactive phosphorus (SRP) (A) and total phosphorus (TP) (B) concentrations at Spring Lake monitoring sites. Legend in panel A also applies to B. Note y-axis scales change between panels.

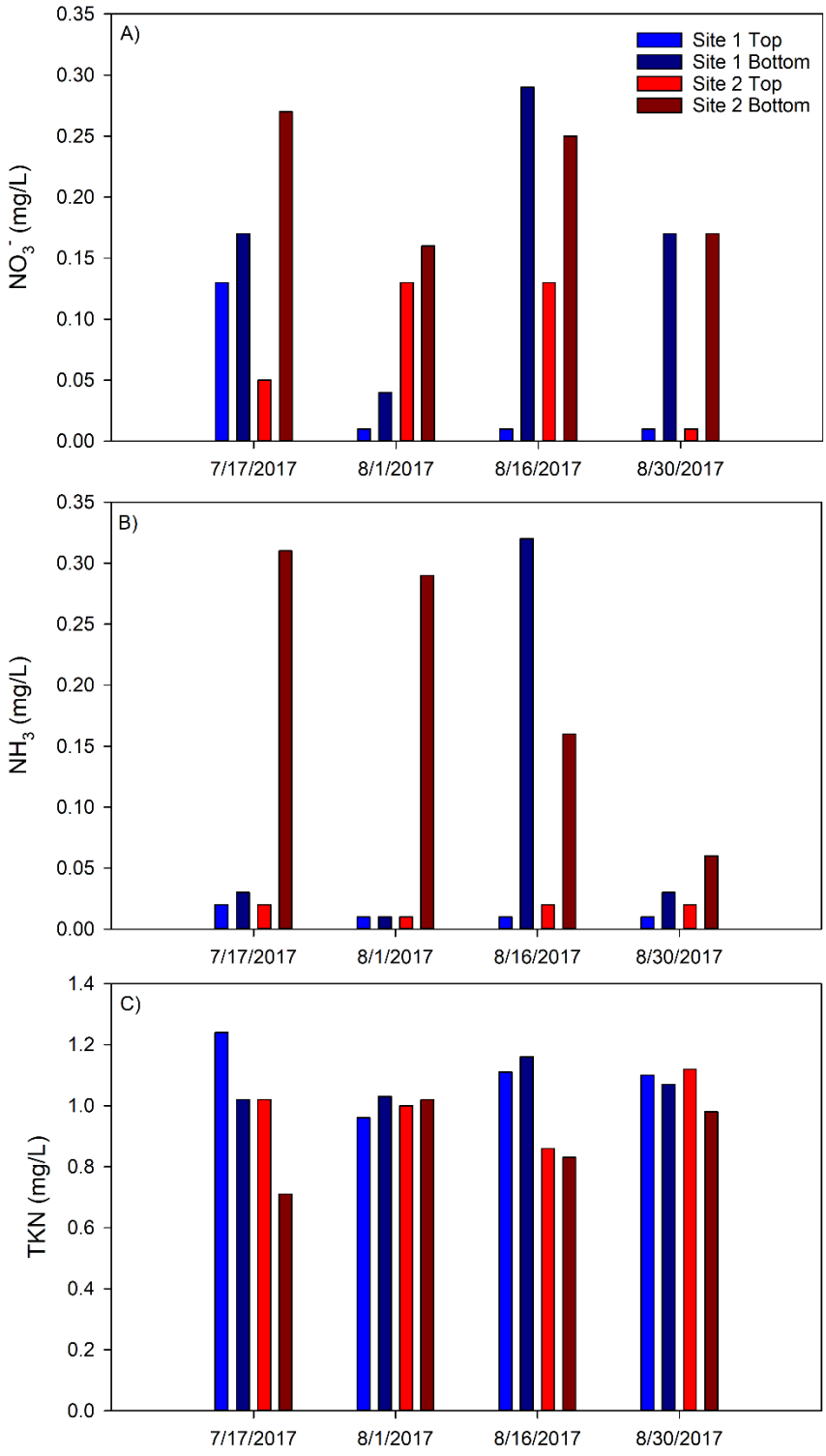

Figure 11. Nitrate (NO_3^-) (A), ammonia (NH_3) (B), and total Kjeldahl nitrogen (TKN) (C) concentrations at Spring Lake monitoring sites. Legend in panel A also applies to B and C. Note y-axis scales change between panels.

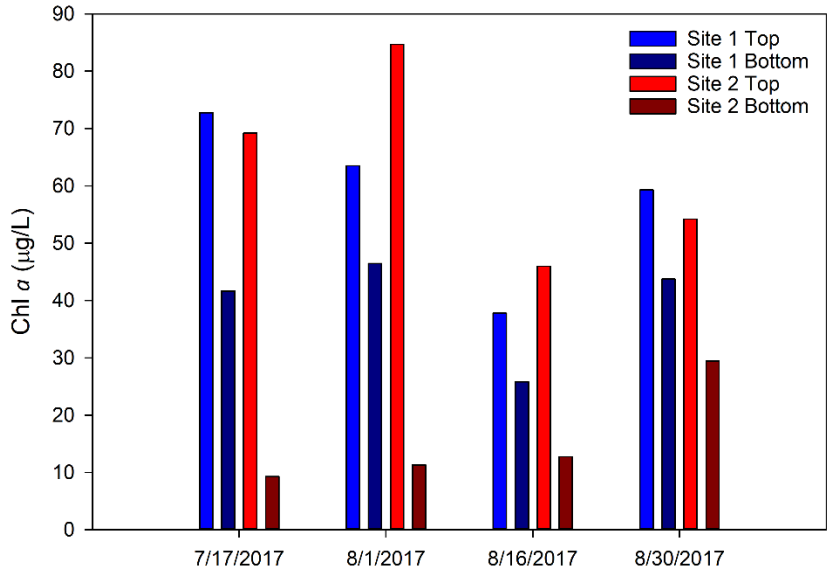

Figure 12. Chlorophyll *a* (Chl *a*) concentrations at Spring Lake monitoring sites.

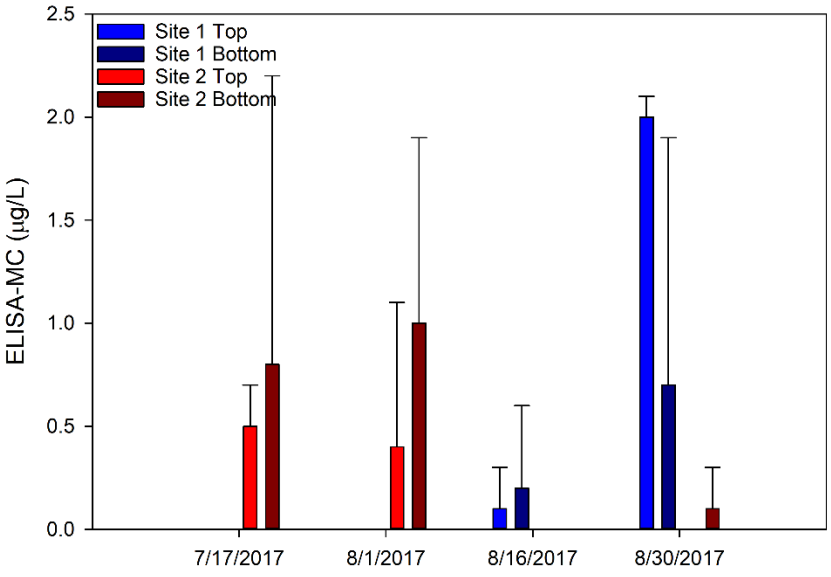

Figure 13. Microcystin (MC) concentrations at Spring Lake monitoring sites as determined by ELISA tube kits.

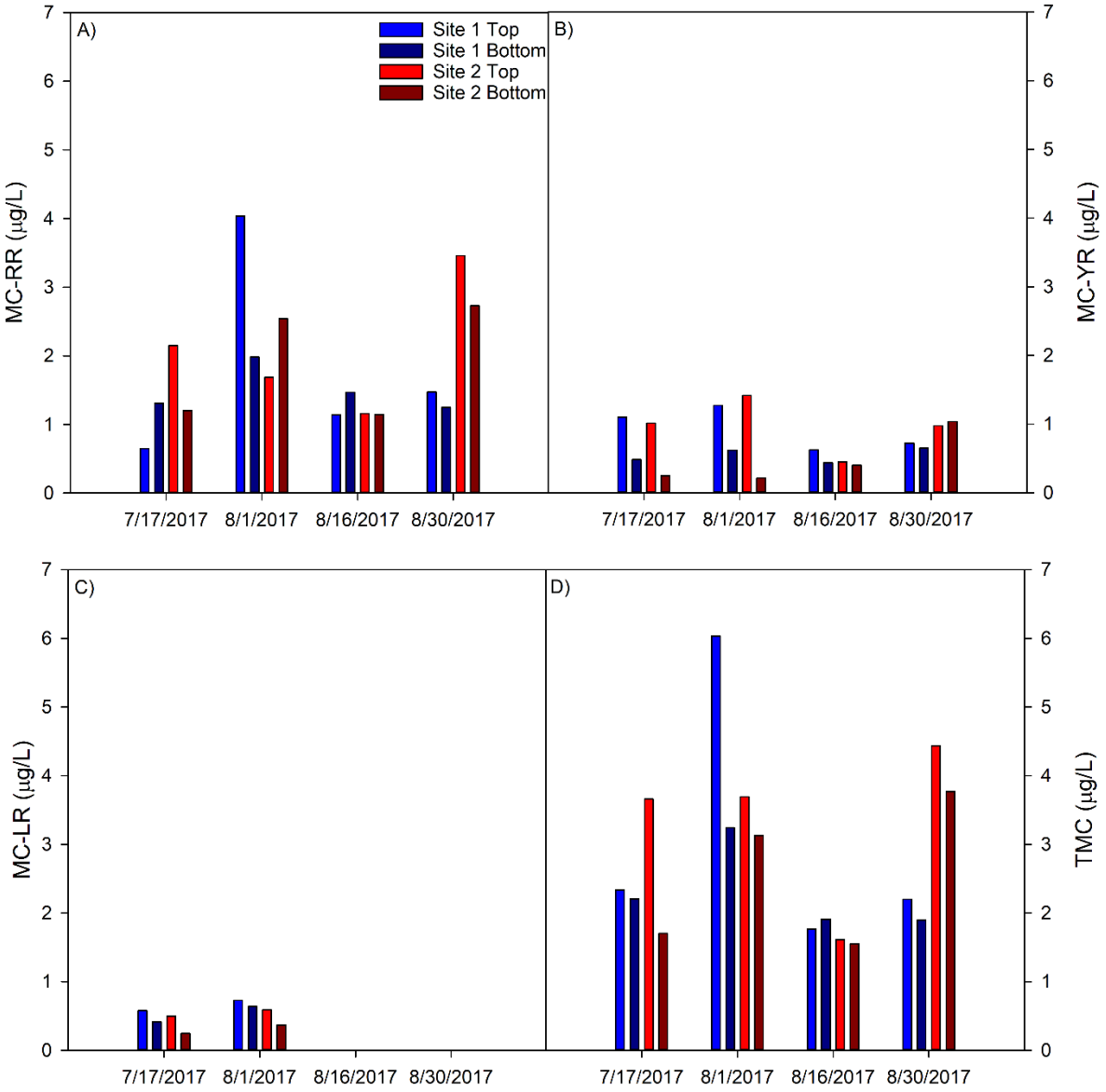

Figure 14. Microcystin (MC) concentrations at Spring Lake monitoring sites as determined by high-performance liquid chromatography (HPLC). Note that y-axis scales between panels are equal. Values in C on 8/16 and 8/30 are 0 µg/L. Total MC (TMC) concentration is the sum of MC-RR, MC-YR, and MC-LR.

Discussion

Tributary Water Quality

In general, most aquatic ecologists and watershed resource managers believe that it is essential to control as much of the external P loading as possible, as this is usually the source of P for internal loading. As long as P continues to enter a lake from the watershed, controlling just internal loading is the equivalent of treating the symptom and not the disease. In opposition, Osgood (2017) argues there are circumstances when it makes little sense to focus on external loading, and that resources are better spent on the control of internal loading to improve lake health.

In the Spring Lake watershed, resources have been devoted largely to controlling internal P loading (through an alum treatment), with little implementation to control external loading. Results from this study provide additional evidence that management of runoff from the watershed will yield long-term benefits to Spring Lake.

Mean TP concentrations during baseflow in Spring Lake tributaries are certainly not excessive, ranging from a high of 35 µg/L, in the upper watershed where agricultural land use dominates, to a low of 15 µg/L. The Spring Lake tributary TP concentrations compare favorably to other watersheds in west Michigan. The mean annual TP concentrations flowing into Mona Lake were 45 µg/L from Little Black Creek and 60 µg/L from Black Creek (Steinman et al. 2006). In the Macatawa watershed, the main tributary to Lake Macatawa averaged about 100 µg/L on an annual basis (Hassett et al. 2018).

However, storm flow TP concentrations tell a different story. Storm events are usually associated with elevated TP concentrations, as the erosive force of storm flow can move P-rich sediments off the land and stream banks (Sharpley et al. 2008). Indeed, mean TP concentrations in Spring Lake tributaries were elevated to between 65 and 125 µg/L. These concentrations are approximately equivalent to the TP concentrations in the lake itself. Comparatively speaking, these storm event TP concentrations are modest compared to the Middle Macatawa River, a heavily agricultural watershed just 25 miles south of the Spring Lake watershed; TP concentrations during storm flow in the Middle Mac range from ~1400 to ~1600 µg/L, a full order of magnitude greater than any tributary in the Spring Lake watershed (Steinman et al. submitted).

Phosphorus Budget

Using the data from our tributary sampling, the prior studies on internal loading, and estimates of other (minor) sources of external loading from Lauber's thesis (1999), we were able to construct an updated P budget for Spring Lake. As a first order estimate, external loading accounts for approximately 71.4% of the TP load to Spring lake, with tributaries accounting for ~65% of that external load. Lauber (1999) estimated that tributaries accounted for 67% of the external load to Spring Lake, with a range from 59% to 78%. She did not estimate internal load.

These estimates are broadly accurate, but there are many uncertainties associated with them. For external loading, we applied Lauber's loading estimates for septage, waterfowl, lawn fertilizer, and shoreland runoff sources, which account for 23% of all the P loads to the lake in our budget (Table 10).

It is very likely that both septage (13.9%) and lawn fertilizer (7.6%) are overestimates because of changes that have occurred since 1999. More homes and businesses, especially in the northern region of the lake (Fruitport area), have replaced septic systems with sanitary sewers, and since 2012, the Michigan Fertilizer Law has restricted P application on residential and commercial lawns. If we assume that the total P load from these two sources was reduced by half, which still may be a conservative estimate, the contributions from tributaries increases from 46% to 52% and internal loading increases from 28.6% to 32%.

The internal loading estimate is also subject to uncertainty. For the purposes of this study, we assumed that sediment release of P occurred over half the year. Prior studies have shown that sediment release of P is very low or non-existent in colder months (Steinman et al. 2009). However, we also assumed that our measured P release rates, based on 4 sites in the middle of the lake, applied throughout the entire lake area; we have not validated that assumption and it is possible that release rates may be higher in shallower regions of the lake, where alum was not applied back in 2005. Hence, internal loading may account for more than 28.6% we estimated here.

Regardless of these uncertainties and caveats, it is clear that tributaries account for the vast majority of the external loading to Spring Lake, and that storm events generate much of the P load. BMPs that keep P in the watershed and detain storm flow are recommended.

Microcystins

The occurrence and intensity of cyanobacterial (blue-green algae) blooms are increasing on a global basis (O'Neill et al. 2012). Both eutrophication and climate warming have been shown to be driving these increases (Moss et al. 2011); of these two factors, eutrophication is believed to be the more significant (Rigosi et al. 2014, Lürling et al. 2017).

MC are the most abundant type of toxins released from cyanobacteria in freshwaters. There are over 100 variants of MCs (Buratti et al. 2017), but the most abundant are MC-LR, MC-YR, and MC-RR. The World Health Organization has established provisional MC guidelines of 1 µg/L for drinking water and 20 µg/L for recreational waters (Chorus and Bartram 1999). MCs are hepatotoxins that are suspected of causing liver cancer (Chen et al. 2016, Harke et al. 2016) and a tumor promoter (Ibelings and Chorus 2007). In addition, MC-LR has been shown to work its way up through the food web, potentially causing harm to humans (Sun et al. 2013, Pham et al. 2018)

The total MC concentrations that we measured in Spring Lake ranged from ~0.1 to 2 µg/L using the ELISA tube kits and from ~1.5 to 6 µg/L when using the more sensitive HPLC. We previously measured MCs in Spring Lake in 2006 (Xie et al. 2012); our HPLC analyses at that time (sampling in both studies was in July and August) revealed much lower total MC concentrations in Spring Lake, with a mean of ~0.06 µg/L.

MC concentrations are influenced by the abundance of cyanobacteria in the water column; the greater the density of cyanobacteria, the greater the MC concentrations. We did not measure the amount of cyanobacteria in either 2006 or 2017, but we did measure Chl *a*, which is a proxy for the total amount of algae in the water. In both 2006 and 2017, Chl a concentrations were similar, ranging from ~30 to 75 µg/L. If the cyanobacteria population composed a greater percentage of the total algal community in

2016, this would account for the higher MC concentrations. Alternatively, changes in lake condition (e.g., related to N) may have resulted in a greater abundance of more toxic strains of cyanobacteria. Our limited sampling does not give us confidence to say definitively the cause of this increase. The key findings are that 1) mid-summer MC concentrations have increased in Spring Lake between 2006 and 2017; and 2) despite the increase, concentrations are still far below the provisional guidelines for recreational use.

Recommendations

Water Quality:

1) The external loading results indicate that Norris Creek contributes the most P load of the sampled tributaries in the Spring Lake watershed. As a consequence, BMPs should target this tributary. In addition, because P concentrations are highest at upstream locations, the location of those P sources should be identified and BMPs designed and implemented at those sources.

2) We previously developed a flow chart that outlines a BMP selection process for the Spring Lake watershed (Steinman et al. 2015); we recommend that the local municipalities revisit this flow chart and begin the process of prioritizing the types and locations of BMPs to most effectively and efficiently control nutrient loading to Spring Lake.

Phosphorus Budget:

3) The P budget should be updated with more recent information, especially regarding septage and lawn fertilizer loads.

4) A watershed computational model (e.g., SWAT) would allow managers to evaluate different scenarios on land use impacts in the watershed. This would take time and money to construct, but ultimately would be a powerful tool for planners and regulators.

Microcystins:

5) The increase in MCs between 2006 and 2017 is of potential concern. MC analysis should become part of future sampling regimes.

Acknowledgments

Funding for this project was provided by the Spring Lake-Lake Board and Progressive AE. We thank Tony Groves and Pam Tyning for their feedback. Xiaomei Su, Emily Kindervater, Kim Oldenborg, Paige Kleindl, Nicole Hahn, Brooke Ridenour, and Rachel Orzechowski contributed many hours of work on field and lab components of this project. Thank you to Brian Scull for completing all P and N nutrient analyses and Kurt Thompson for creating site maps. We additionally thank the lab of Liqiang Xie at Nanjing Institute of Geography and Limnology, Chinese Academy of Sciences for assisting with HPLC analysis.

Literature Cited

Brennan, A.K., Hoard, C.J., Duris, J.W., Ogdahl, M.E., and Steinman, A.D., 2015, Water quality and hydrology of Silver Lake, Oceana County, Michigan, with Emphasis on lake response to nutrient loading, 2012–14. U.S. Geological Survey Scientific Investigations Report 2015–5158, 75 p., http://dx.doi.org/10.3133/sir20155158.

Buratti F.M., Manganelli M., Vichi S., Stefanelli M., Scardala S., Testai E. and E. Funari. 2017. Cyanotoxins: producing organisms, occurrence, toxicity, mechanism of action and human health toxicological risk evaluation. Archives of Toxicology 91: 1049-1130.

Chen L., Chen J., Zhang X. P. and P. Xie. 2016. A review of reproductive toxicity of microcystins. Journal of Hazardous Materials 301: 381-399.

Chorus I. and J. Bartram. 1999. Toxic cyanobacteria in water: a guide to their public health consequences, monitoring and management. CRC Press.

Chu, X, and A.D. Steinman. 2009. Event and Continuous Hydrologic Modeling with HEC-HMS. ASCE's Journal of Irrigation and Drainage Engineering 135: 119-124.

Harke M.M., Steffen J, Gobler CJ, Otten TG, Wilhelm SW, Wood SA, and HW Paerl. 2016. A review of the global ecology, genomics, and biogeography of the toxic cyanobacterium, Microcystis spp. Harmful Algae 54: 4-20.

Hassett M., Oudsema M., and A.D. Steinman. 2018. Project Clarity Annual Monitoring Report. Available at: https://www.gvsu.edu/cms4/asset/DFC9A03B-95B4-19D5-F96AB46C60F3F345/project_clarity_final_report2017.pdf

Ibelings B.W. and I. Chorus. 2007. Accumulation of cyanobacterial toxins in freshwater “seafood” and its consequences for public health: A review. Environmental Pollution 150: 177-192.

Kramer B.J., Davis T.W., Meyer K.A., Rosen B.H., Goleski J.A., Dick G.J., Oh G., and C.J. Gobler. 2018. Nitrogen limitation, toxin synthesis potential, and toxicity of cyanobacterial populations in Lake Okeechobee and the St. Lucie River Estuary, Florida, during the 2016 state of emergency event. PloS One 13(5): e0196278.

Lauber, T. 1999. Can the big bayou be saved? Water quality assessment and management recommendations for Spring Lake watershed, Ottawa and Muskegon Counties, Michigan. Thesis for the Degree of M.S. Michigan State University.

Lürling, M., Van Oosterhout, F., and E. Faassen. 2017. Eutrophication and warming boost cyanobacterial biomass and microcystins. Toxins. 9: 64.

Moss, B., Kosten, S., Meerhoff, M., Battarbee, R.W., Jeppesen, E., Mazzeo, N., Havens, K., Lacerot, G., Liu, Z., De Meester, L. and H. Paerl. 2011. Allied attack: climate change and eutrophication. Inland Waters 1: 101-105.

O’Neil, J.M., Davis, T.W., Burford, M.A. and C.J. Gobler. 2012. The rise of harmful cyanobacteria blooms: the potential roles of eutrophication and climate change. Harmful Algae 14: 313-334.

Osgood, R.A. 2017. Inadequacy of best management practices for restoring eutrophic lakes in the United States: Guidance for policy and practice. Inland Waters 7: 401-407.

Otten, T.G., Xu, H., Qin, B., Zhu, G., and H.W. Paerl. 2012. Spatiotemporal Patterns and Ecophysiology of Toxigenic Microcystis Blooms in Lake Taihu, China: Implications for Water Quality Management. Environmental Science & Technology 46: 3480-3488.

Pham T.-L. and M. Utsumi. 2018. An overview of the accumulation of microcystins in aquatic ecosystems. Journal of Environmental Management 213: 520-529.

Rigosi, A., Carey, C.C., Ibelings, B.W. and J.D. Brookes. 2014. The interaction between climate warming and eutrophication to promote cyanobacteria is dependent on trophic state and varies among taxa. Limnology and Oceanography 59: 99-114.

Sharpley, A.N., Kleinman, P.J., Heathwaite, A.L., Gburek, W.J., Folmar, G.J. and J.P. Schmidt. 2008. Phosphorus loss from an agricultural watershed as a function of storm size. Journal of Environmental Quality 37: 362-368.

Steinman, A.D., Rediske, R., and K.R. Reddy. 2004. The importance of internal phosphorus loading to Spring Lake, Michigan. Journal of Environmental Quality 33: 2040-2048.

Steinman, A.D., Rediske, R., Chu, X., Denning, R., Nemeth, L., Uzarski, D., Biddanda, B., and M. Luttenton. 2006. An environmental assessment of an impacted, urbanized watershed: the Mona Lake Watershed, Michigan. Archiv für Hydrobiologie 166: 117-144.

Steinman, A.D. and M. Ogdahl. 2008. Ecological effects following an alum treatment in Spring Lake, Michigan. Journal of Environmental Quality 37: 22-29.

Steinman, A.D., Chu, X., and M. Ogdahl. 2009. Spatial and temporal variability of internal and external phosphorus loads in an urbanizing watershed. Aquatic Ecology 43: 1-18.

Steinman, A.D. and M.E. Ogdahl. 2012. Macroinvertebrate response and internal phosphorus loading in a Michigan Lake following alum treatment. Journal of Environmental Quality 41: 1540-1548.

Steinman A.D., Isely E.S. and K. Thompson. 2015. Stormwater runoff to an impaired lake: impacts and solutions. Environmental Monitoring and Assessment. 187: 549.

Steinman A.D., Hassett M.C., Oudsema M. and R. Rediske. 2018. Alum efficacy 11 years following treatment: Phosphorus and macroinvertebrates. Lake and Reservoir Management 34: 167-181.Steinman A.D., Hassett M.C., and M. Oudsema. Submitted. Effectiveness of Best Management Practices to Reduce Phosphorus Loading to a Highly Eutrophic Lake. International Journal of Environmental Research and Public Health.

Su X., Xue Q., Steinman A., Zhao Y., and L. Xie. 2015. Spatiotemporal Dynamics of Microcystin Variants and Relationships with Environmental Parameters in Lake Taihu, China. Toxins 7, 3224.

Sun X., Wu L., Ji J., Jiang D., Zhang Y., Li Z., Zhang G. and H. Zhang. 2013. Longitudinal surface plasmon resonance assay enhanced by magnetosomes for simultaneous detection of Pefloxacin and Microcystin-LR in seafoods. Biosensors and Bioelectronics 47: 318-323.

U.S. EPA 1993 Methods for Chemical Analysis of Inorganic Substances in Environmental Samples. EPA600/4-79R-93-020/100.

USEPA. 2011. 2012 National Lakes Assessment. Field Operations Manual. EPA 841-B-11-003. USEPA, Washington, DC.

Xie L., Rediske R.R., Hong Y., O'Keefe J., Gillett N, Dyble J. and A.D. Steinman. 2012. The role of environmental parameters in the structure of phytoplankton assemblages and cyanobacteria toxins in two hypereutrophic lakes. Hydrobiologia 691: 255-268.

Appendix A.

Tables A.1 and A.2

Figures A.1 – A.8

Table A1. Results of best-fit modeling for Spring Lake tributary sites. Stage-Pressure models were derived from field-measured creek stage and automated sensor-collected pressure time series data. Discharge-stage and discharge-pressure models were derived from sensor-collected pressure, modeled stage, and modeled discharge time series data. Site V1 was found to have a bi-linear stage-pressure trend, separated approximately by stage at <40 cm (V1 low stage) and >40 cm (V1 high stage); separate models were derived and are reported below.

Site	**Stage-Pressure Model**		**Discharge-Stage Model***		**Discharge-Pressure Model***	
	Equation: y=stage (cm) x=pressure (kPa)	R^2	Equation: y=discharge (m^3) x=stage (cm)	R^2	Equation: y=discharge (m^3) x=pressure (kPa)	R^2
S1	$y=-0.2813x^2+12.394x-1.7386$	0.8699	**$y=0.0002x^2-0.0086x+0.177$**	**0.6547**	$y=0.0259x^2-0.1041x+0.2132$	0.6030
WH1	$y=9.4357x+2.5904$	0.8900	$y=0.0003x2+0.0004x+0.0238$	0.7678	**$y=0.0445x^2-0.0421x+0.0637$**	**0.8033**
V1 low	$y=55.211*\ln(x)-78.707$	0.6025	$y=1E-06^{0.4274x}$	0.9458	**$y=-0.0237x^2+0.4076+1.5153$**	**0.9703**
V1 high	$y=-0.0949x^2+11.307x-1.828$	0.9968	$y=0.0004x^2-0.0408x+0.9829$	0.9607	**$y=0.039x^2-0.3514x+0.7758$**	**0.9415**
N1	$y=-0.5429x^2+11.567+22.758$	0.5706	$y=0.0129x^{1.0333}$	0.5413	**$y=0.4434x^{0.5817}$**	**0.6118**
R1	$y=10.746x+1.5283$	0.9805	$y=0.0048x^{1.2785}$	0.8216	**$y=0.124x^{1.1135}$**	**0.8529**
N2	$y=-0.6237x^2+13.985x-3.1998$	0.9242	**$y=0.0001x^2+0.0115x+0.0841$**	**0.8002**	$y=0.0079x^2+0.1658x+0.0331$	0.7935
N3	$y=14.003x^{0.6934}$	0.7889	**$y=0.014x^{0.8163}$**	**0.2654**	$y=0.1245x^{0.5342}$	0.1788

Table A2. Muskegon County Airport precipitation records across thirty years from 1988-2018. Hourly precipitation records were downloaded during August 2018 from NCEI local climate dataset and summed into months. Monthly totals are color-coded in 3” precipitation ranges to improve readability (see legend).

Year	Jan	Feb	Mar	Apr	May	Jun	Jul	Aug	Sep	Oct	Nov	Dec
1988	2.89	1.66	1.95	3.83	0.43	0.47	1.65	3.11	5.92	4.79	6.58	2.82
1989	1.61	1.04	1.92	0.72	4.64	0.89	1.36	4.86	2.41	1.58	2.92	1.90
1990	2.34	1.74	2.41	2.01	6.48	3.63	1.26	1.22	3.79	4.36	5.31	2.60
1991	1.36	0.75	4.40	3.56	3.52	3.84	3.31	3.88	3.32	7.33	4.25	1.82
1992	1.36	1.33	2.30	3.30	0.33	1.50	2.68	1.97	3.54	2.46	6.26	2.68
1993	2.62	0.83	1.61	4.88	2.26	4.40	3.87	6.40	4.59	1.66	2.00	1.10
1994	2.66	2.65	1.34	2.38	1.28	4.99	2.46	5.22	2.91	2.16	3.81	0.99
1995	2.84	1.30	1.79	3.47	1.83	0.71	2.66	3.55	0.99	3.65	4.85	1.88
1996	1.47	1.58	1.22	2.47	3.37	4.13	1.77	1.11	2.07	2.80	1.23	1.66
1997	2.01	3.36	1.03	1.82	2.47	3.48	3.00	3.05	3.35	1.44	2.75	1.28
1998	2.72	1.58	3.89	1.81	1.91	1.63	1.03	2.98	3.87	4.70	2.49	1.49
1999	2.46	1.61	0.45	4.74	6.11	4.27	3.44	3.71	2.86	0.85	0.96	3.08
2000	1.25	1.17	1.40	6.16	8.79	3.25	3.45	3.26	6.23	2.35	4.33	1.01
2001	0.87	4.00	0.70	6.43	6.99	2.81	2.58	4.59	5.55	8.53	2.53	1.78
2002	0.75	2.31	1.98	5.50	3.21	6.83	3.49	14.44	4.45	4.42	2.20	1.32
2003	0.59	0.40	2.47	4.86	7.51	2.29	12.14	5.27	7.34	3.21	12.68	2.88
2004	2.87	1.17	8.61	3.93	27.54	11.60	3.80	9.48	0.35	8.74	5.28	5.58
2005	6.69	4.59	3.04	0.58	5.59	4.18	4.95	9.55	10.61	0.70	14.10	3.08
2006	5.93	3.71	14.26	5.62	8.64	3.66	13.62	3.97	8.14	10.23	4.93	5.76
2007	2.95	2.18	6.13	7.65	4.31	4.25	3.99	14.30	9.29	4.29	0.75	4.39
2008	7.07	4.65	6.27	6.04	4.05	17.38	10.33	3.54	13.40	6.00	4.67	9.00
2009	1.75	6.47	5.74	8.31	3.40	5.55	2.30	12.42	7.60	11.14	3.82	4.54
2010	1.02	2.12	1.91	4.48	5.20	12.45	9.14	8.53	17.64	4.72	2.27	3.22
2011	5.08	4.35	6.26	11.04	6.15	7.40	12.62	20.43	7.69	7.70	6.11	4.44
2012	5.42	3.72	7.78	4.36	3.40	8.43	8.36	2.46	1.29	16.60	0.92	5.70
2013	13.28	6.71	2.46	18.21	13.57	12.39	4.14	3.88	4.82	9.30	5.04	5.11
2014	4.61	3.35	2.82	5.95	8.18	15.63	15.64	6.10	4.86	5.54	6.92	3.11
2015	2.35	2.77	2.13	4.77	7.41	7.17	16.42	4.85	9.39	4.12	5.99	7.60
2016	3.30	3.65	11.80	3.27	3.61	6.60	16.51	6.33	15.15	8.68	4.36	5.33
2017	5.84	4.72	4.38	7.68	2.59	10.16	3.99	2.72	0.95	15.21	4.34	4.62
2018	5.26	7.81	2.41	6.12	10.07	4.67	2.67					

Legend:
0"-3"
3"-6"
6"-9"
9"-12"
12"-15"
>15"

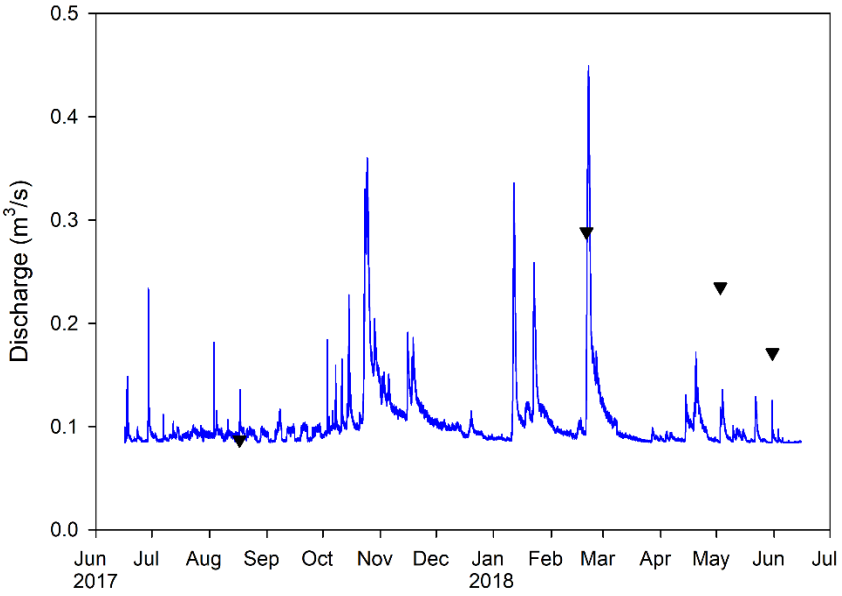

Figure A1. S1 hydrograph model from June 16, 2017 – June 15, 2018. Inverted triangles indicate *in situ* storm sampling events.

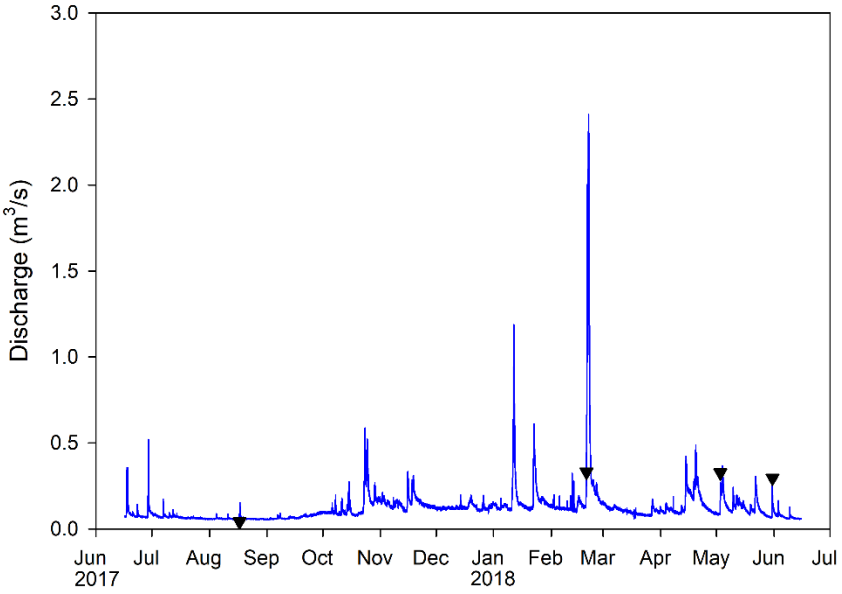

Figure A2. WH1 hydrograph model from June 16, 2017 – June 15, 2018. Inverted triangles indicate *in situ* storm sampling events.

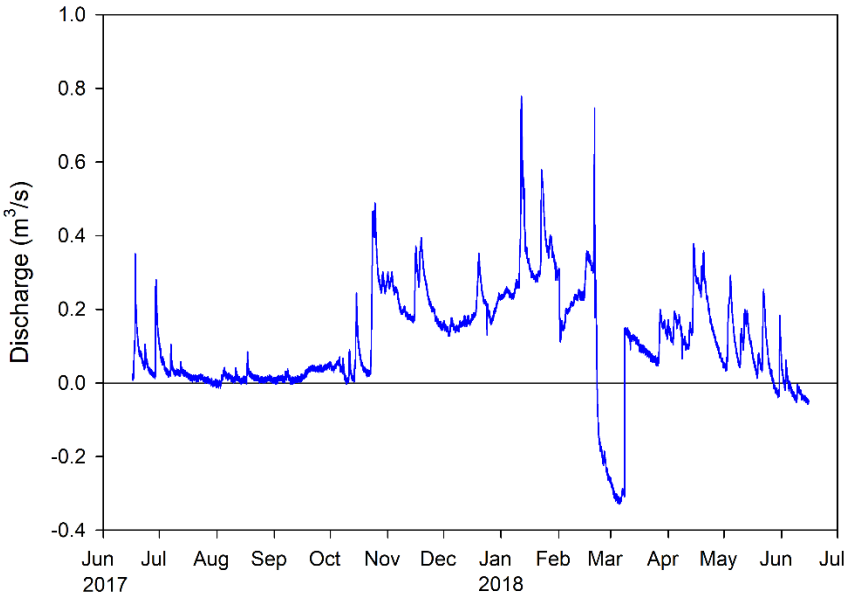

Figure A3. V1 (low stage) hydrograph model from June 16, 2017 – June 15, 2018. Low values from Feb 20 – Mar 8 are because stage was knocked over, exact cause unknown. Discovered in creek downstream of sampling site during Mar 8 baseflow, determined to not be broken, and reinstalled.

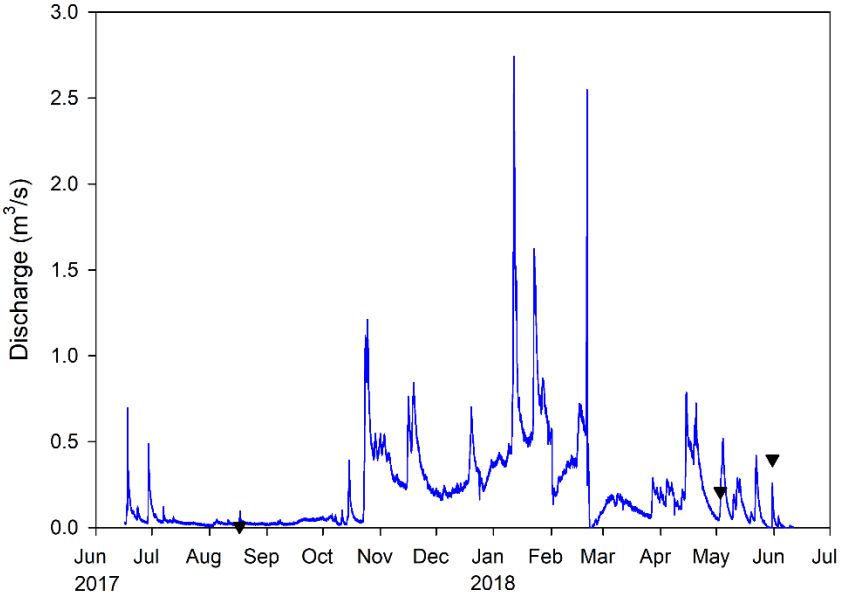

Figure A4. V1 (high stage) hydrograph model from June 16, 2017 – June 15, 2018. Inverted triangles indicate *in situ* storm sampling events.

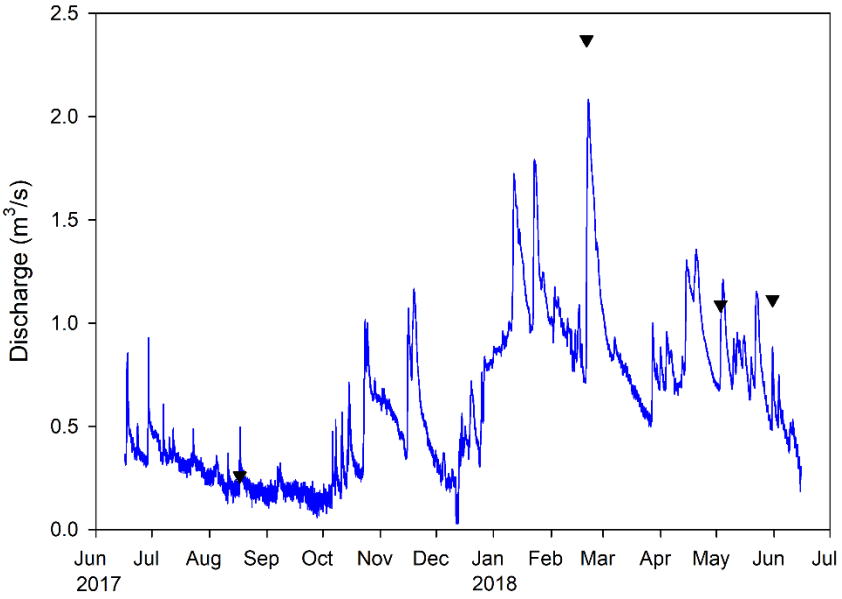

Figure A5. N1 hydrograph model from June 16, 2017 – June 15, 2018. Inverted triangles indicate *in situ* storm sampling events.

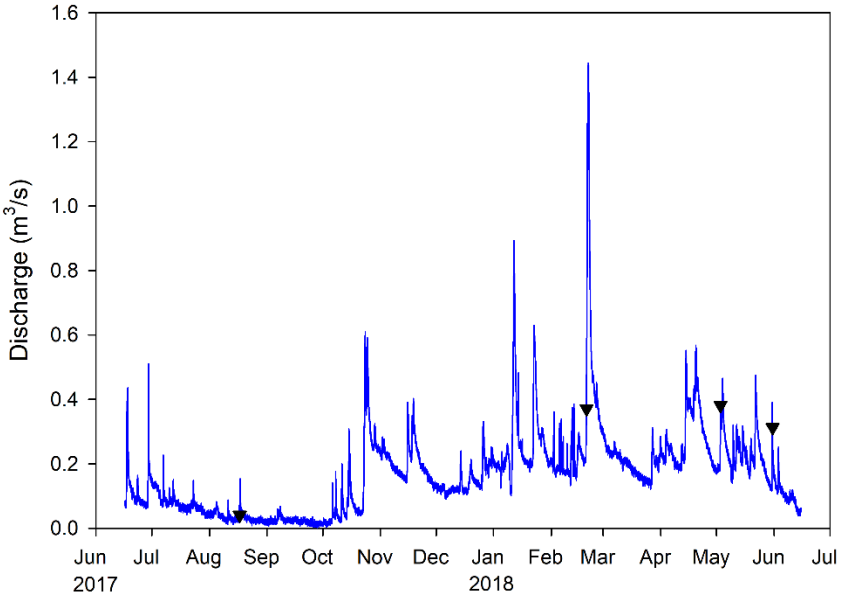

Figure A6. R1 hydrograph model from June 16, 2017 – June 15, 2018. Inverted triangles indicate *in situ* storm sampling events.

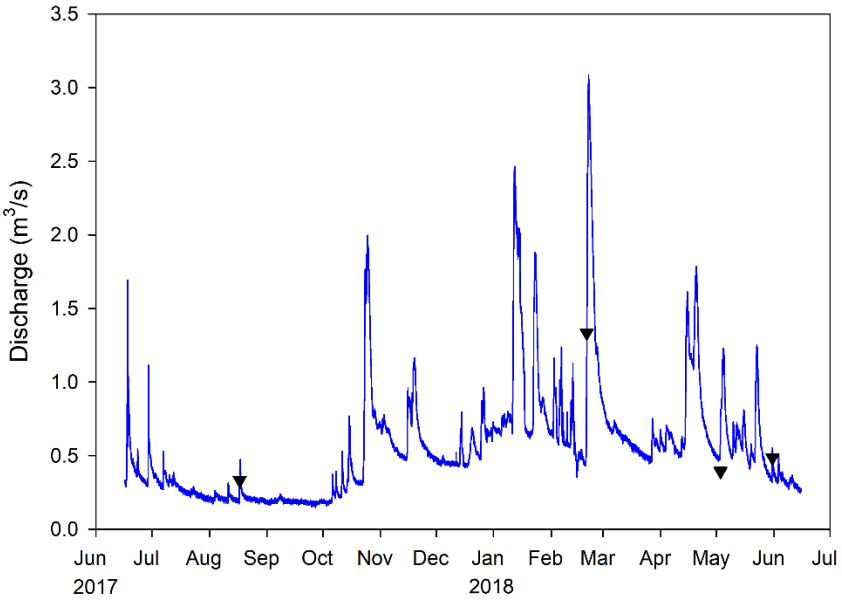

Figure A7. N2 hydrograph model from June 16, 2017 – June 15, 2018. Inverted triangles indicate *in situ* storm sampling events.

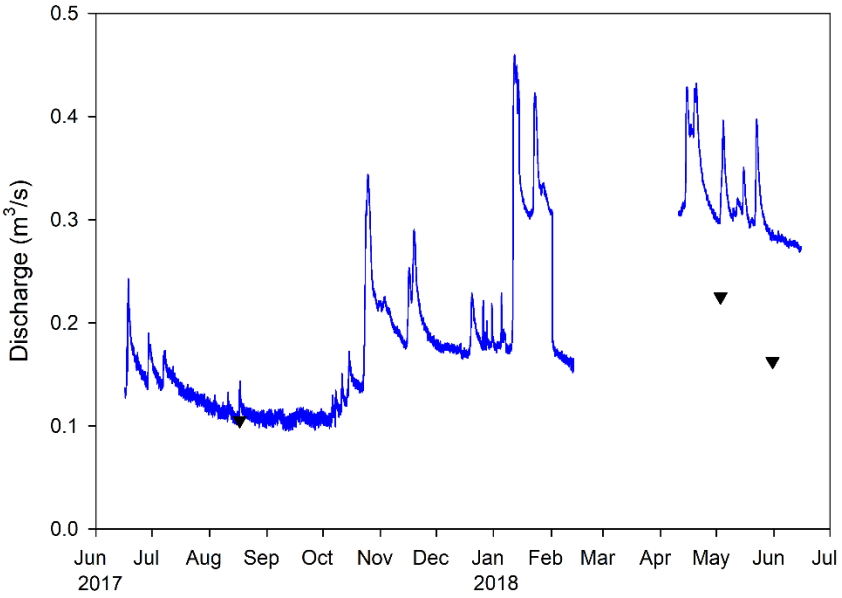

Figure A8. N3 hydrograph model from June 16, 2017 – June 15, 2018. Inverted triangles indicate *in situ* storm sampling events.